MafB is critical for glucagon production and secretion in pancreatic α-cells *in vivo*.

(膵α細胞において、MafB はグルカゴン産生
および分泌に重要である)

2017

筑波大学グローバル教育院

School of the Integrative and Global Majors in University of Tsukuba

Ph.D. Program in Human Biology

Megumi Katoh

筑　波　大　学

University of Tsukuba

博　士　（人間生物学）　学　位　論　文

Ph.D. dissertation in Human Biology

MafB is critical for glucagon production and secretion

in pancreatic α-cells *in vivo*.

ABSTRACT

MafB (v-maf musculoaponeurotic fibrosarcoma oncogene homolog B) transcription factor is expressed in pancreatic α- and β-cells during development but becomes exclusive to α-cells in adult rodents. Previous studies in *Mafb*-null ($Mafb^{-/-}$) mice revealed a marked reduction in α- and β-cell numbers throughout embryonic development. However, $Mafb^{-/-}$ mice die soon after birth, restricting postnatal analyses of MafB function in the pancreas. Thus, I generated two *Mafb* conditional knockout mouse models: endocrine cell-specific ($Mafb^{\Delta Endo}$) and tamoxifen-dependent ($Mafb^{\Delta TAM}$) mutant mice. The $Mafb^{\Delta Endo}$ mice exhibited a reduced population of insulin$^+$ and glucagon$^+$ cells on postnatal day 0 but recovered the insulin$^+$ cell population by 8 weeks of age. In contrast, the Arx$^+$ α-cell population and glucagon expression remained decreased even in adulthood. The $Mafb^{\Delta TAM}$ mice, in which *Mafb* was deleted after pancreas maturation, also demonstrated diminished glucagon$^+$ cells and glucagon content without an effect on β-cells. The $Mafb^{\Delta Endo}$ mice displayed an increased Arx$^+$/pancreatic polypeptide$^+$ cell population as compensation for the decreased Arx$^+$/glucagon$^+$ cell population. Furthermore, according to the gene expression analyses of both $Mafb^{\Delta Endo}$ and $Mafb^{\Delta TAM}$ islets, MafB is a key regulator of glucagon expression in α-cells. Finally, both mutants failed to respond to arginine, likely due to impaired arginine transporter gene expression and glucagon production ability. Taken together, my findings reveal that MafB is critical for the functional maintenance of mouse α-cells *in vivo*, including glucagon production and secretion, as well as in development.

ACKNOWLEDGMENTS

First and foremost, I would like to show my greatest appreciation to my research supervisor, Prof. Satoru Takahashi, and my academic supervisor, Prof. Akira Shibuya, for taking a chance on me and giving me the opportunity to carry out my thesis in the Anatomy and Embryology Laboratory, guiding me throughout this journey, and providing me with their continuous support and understanding.

I owe a very important debt to Yunshin Jung, my dearest friend, and mentor both inside and outside the lab. Without her generous guidance and persistent support, this thesis would not have been possible. Her willingness to give her precious time so generously has been very much appreciated. I am beyond words for what she has done for me.

My sincere gratitude also goes to all present and former members of the Anatomy and Embryology Laboratory, especially Prof. Hisashi Oishi and Dr. Takashi Kudo for all the support and advice they gave me; Chioma M. Ugboma, Masami Ojima, Dr. Miki Shimbo, Akihiro Kuno, Asuka Tagami, Risa Fujii, Sayaka Fuseya, and Riku Suzuki for the technical assistance; Dr. Ryusuke Koshida for the meticulous comments on my research paper; and Yukiyo Ida for the secretarial services.

Special thanks go to Dr. Shosei Yoshida, and Drs. Kunio Kitamura and Ken-ichirou Morohashi for their generous gift of the *Ngn3*-Cre transgenic mice and rabbit anti-Arx antibody, respectively.

I would like to extend my appreciation to my dissertation committee, Prof. Osamu Ohneda, Prof. Akira Shibuya, and Drs. Seiya Mizuno and Tilo Kunath, for their constructive and insightful comments and suggestions of my thesis.

I am also very grateful to all the faculty members of the Human Biology Program and the staffs at the SIGMA office, for their assistance throughout my Ph.D. study.

Last, but not least, I would like to say a heartfelt thank you to my family, my parents, Masaya and Satomi, and my sister, Manami, for always believing in me, providing me with unfailing love and support throughout my study and through the process of writing this thesis. I also thank all my friends for their enthusiastic encouragement and precious friendship. This accomplishment would not have been possible without them. Thank you.

Megumi Katoh

TABLE OF CONTENTS

LIST OF FIGURES

CHAPTER 1:

INTRODUCTION

1-1. Pancreas structure and function

The pancreas is a secretory organ containing two major glands: an exocrine gland for digestive enzymes and an endocrine gland for pancreatic hormones. The endocrine pancreas is composed of small clusters of cells called the islets of Langerhans, which include insulin-producing β-cells, glucagon-producing α-cells, somatostatin-producing δ-cells, pancreatic polypeptide (PP)-producing PP-cells, and ghrelin-producing ε-cells. In particular, insulin and glucagon regulate glucose homeostasis: blood glucose levels decrease in response to insulin and increase in response to glucagon. The failure of this hormonal balance due to β-cell dysfunction causes hyperglycemia, which is a key feature of diabetes that often accompanies α-cell impairment (1–3). Therefore, understanding pancreatic α- and β-cell biology contributes deeper insight into hormonal regulation.

1-2. Pancreas development and transcription factors

Pancreatic islet development and specification, including α- and β-cell differentiation, are governed by various important transcription factors (4, 5). For example, Pdx1, which is a pancreatic progenitor marker, drives all pancreatic lineages. Ngn3, which is an endocrine progenitor marker, initiates pancreatic endocrine cell fates. Pax4 and Arx promote β- and α-cell specification and differentiation, respectively (4, 5). Finally, MafA is required for β-cell maturation and functional maintenance (6–8), and MafB plays a decisive role in α-cells, although MafB is also involved in both α- and β-cell development during pancreas morphogenesis (9–11).

1-3. Maf transcription factors

Maf proteins belong to a large class of transcription factors originally described as viral oncogenes. They are characterized by the presence of a basic leucine zipper (b-Zip) domain and the ability to bind to Maf Recognition Element (half-MARE; TGCTGA), a specific binding motif for Maf transcription factors (12), either as homodimers or heterodimers with other b-Zip proteins. The best-characterized Maf transcription factors expressed in the pancreas are MafB (v-maf musculoaponeurotic fibrosarcoma oncogene homolog B) and MafA.

MafB is first detected in the mouse embryonic pancreas from embryonic day 10.5 (7, 9) and becomes exclusively confined to α-cells within 2 weeks of birth (8). In α-cells, MafB activates glucagon gene expression through the G1 element of the glucagon promoter region located between -77 and -51 base pairs relative to the transcription start site (9); hence, glucagon is generally considered an α-cell marker (4, 5). Whereas, in β-cells, MafB and MafA are expressed in a unique temporal manner and are required at distinct stages with MafB being required during development and MafA in adults (7, 8). MafB is critical for β-cell maturation in the late phase of pancreas morphogenesis through the regulation of key β-cell genes such as *Insulin*, *Pdx1*, and *Mafa* (8). According to the gene expression profile analysis by Artner *et al.*, MafB also activates gene involved in mature β-cell function, including those significant to glucose sensing, vesicle maturation, Ca^{2+} signaling, and insulin secretion (8). In contrast, the gene expression of transcription factors associated with β-cell differentiation were unaffected in the *Mafb* knockout ($Mafb^{-/-}$) mice, supporting a role for MafB in the late events essential to β-cell maturation and not in the early β-cell development including β-cell specification and lineage commitment

steps (8). Interestingly, MafA controls many genes first regulated by MafB in adult mice when MafB in silenced (8). However, MafA is solely required for glucose-stimulated insulin secretion in adult β-cells and is not involved in islet cell development (6).

1-4. *Mafb* deficient mice

Previous studies have demonstrated that *Mafb*$^{-/-}$ mouse embryos exhibit reduced α- and β-cell numbers and a delayed onset of insulin expression in β-cells, indicating that MafB plays a role in α- and β-cell differentiation (11). However, because these *Mafb*$^{-/-}$ mice were neonatal lethal due to a defective respiratory rhythm (13), the postnatal function of MafB in pancreatic islets remains unknown. According to a recent study investigating pancreas-wide *Mafb*-deficient (*Mafb*$^{\Delta panc}$) mice, the number of insulin^{+} (Ins^{+}) and glucagon^{+} (Glu^{+}) cells was reduced on postnatal day 1 in neonates (10). Interestingly, both cell types were restored by 2 weeks of age in these mutants, rendering α-cells that were dysfunctional in response to low glucose levels and arginine stimulation *in vitro* (10). These results suggest that MafB is required only for the maintenance of α-cell function but not for glucagon production per se, implying that glucagon expression is compensated by other factors. Given that MafB is a glucagon gene activator (9) and is heavily enriched in mature α-cells (14), these results were intriguing. Additionally, frequent reports of diabetic patients displaying abnormal glucagon regulation highlight the importance of understanding α-cell physiology (1–3).

1-5. Overview and Objectives

Understanding the pancreatic islet cell development and fictional maintenance is essential to provide knowledge in designing novel treatments for diseases related to the pancreas (e.g., type 1 and 2 diabetes). The large Maf transcription factor, MafB, has been shown to be necessary for α- and β-cell terminal differentiation and functional maturation (9, 11, 15). Interestingly, MafB continues to be expressed in the mature α-cells and therefore could play an additional role in α-cell maintenance throughout life (8).

The following chapters in my thesis aim to discover the role of MafB in the postnatal pancreas. **The goal of these experiments is (1) to determine the role of MafB in early postnatal development of islet cells and (2) to describe the effect of MafB loss after islet cell maturation.** Because *Mafb*$^{-/-}$ mice are neonatal lethal, to confirm the postnatal role of MafB in pancreatic islet cells, I generated two types of conditional knockout mice: endocrine cell-specific *Mafb* knockout (*Mafb*$^{\Delta Endo}$) and tamoxifen (TAM)-dependent *Mafb* knockout (*Mafb*$^{\Delta TAM}$) mice.

Here, I investigate an alternative *in vivo* role of MafB in postnatal pancreatic α-cells. Both the *Mafb*$^{\Delta Endo}$ and *Mafb*$^{\Delta TAM}$ mice failed to express glucagon in α-cells, resulting in low basal plasma glucagon levels, which do not recover over time. Moreover, the *Mafb* deficiency disrupted glucagon secretory responses to α-cell stimuli in both mutants. Therefore, MafB is critical for glucagon production during α-cell development and α-cell functional maintenance in adult mice.

CHAPTER 2:

The role of MafB in α- and β-cell development

2-1. Purpose

According to previous studies, the function of transcription factor MafB in embryonic pancreas development has been extensively explored and shown to be important for α- and β-cell differentiation (9, 11, 15). However, studies of MafB in the postnatal pancreas could not be conducted because *Mafb*$^{-/-}$ mice die immediately after birth (13). In this study, I analyzed the mouse model with a conditional *Mafb* knockout in the endocrine cells to determine the postnatal function of MafB in the pancreas.

2-2. Results

Embryonic deletion of *Mafb* in endocrine cells results in postnatal decreases in both Ins^{+} and Glu^{+} cell populations.

To enable postnatal examination, I selected *Neurogenin3* (*Ngn3*)-Cre transgenic mice to specifically delete *Mafb* in the endocrine cells. *Ngn3*-Cre mice express Cre recombinase in all endocrine cell types in the pancreatic islet during embryonic development (16). To verify the Cre recombination activity and specificity of *Ngn3*-Cre mice, these mice were crossed with Cre-reporter mice, R26GRR. R26GRR mice exhibits green fluorescence (EGFP) ubiquitously before, and red fluorescence (tdsRed) exclusively after Cre recombination (17). Pancreas sections from R26GRR::*Ngn3*-Cre mice showed that tdsRed was expressed only in the pancreatic endocrine cells and not in the exocrine cells, thus confirming the high specificity of Cre recombination (Fig. 2.1).

To address the physiological function of MafB in postnatal pancreatic islets, *Ngn3-Cre* mice were then crossed with *Mafb* floxed (*Mafb*$^{f/f}$) mice to generate endocrine cell-specific *Mafb* deficient mutant, *Mafb*$^{f/f}$::*Ngn3*-Cre (*Mafb*$^{\Delta Endo}$) mice. I first performed immunohistochemical studies on pancreatic sections to explore the effects of the *Mafb* loss on the postnatal development of pancreatic endocrine cells by examining insulin and glucagon protein expression (Fig. 2.2A). On postnatal day 0 (P0), the fraction of insulin$^+$ (Ins$^+$) and glucagon$^+$ (Glu$^+$) cells in the *Mafb*$^{\Delta Endo}$ islets was significantly lower than that in the *Mafb*$^{f/f}$ control mice (Fig. 2.2A - C; Control vs. *Mafb*$^{\Delta Endo}$; Ins$^+$, 100 ± 6.9 vs. 25.9 ± 4.3%; Glu$^+$, 100 ± 10.0 vs. 10.7 ± 2.3%). Interestingly, the reduced population of Ins$^+$ cells in the *Mafb*$^{\Delta Endo}$ pancreata recovered to near control levels as the mice aged (Fig. 2.2A and B; Control vs. *Mafb*$^{\Delta Endo}$; 3 W, 100 ± 2.6 vs. 65.4 ± 3.1%; 8 W, 100 ± 2.5 vs. 89.9 ± 4.0%; 20 W, 100 ± 1.8 vs. 92.0 ± 2.2%). However, compared with that in the control groups, the fraction of Glu$^+$ cells in the *Mafb*$^{\Delta Endo}$ islets remained significantly reduced throughout postnatal development until 20 weeks of age (Fig. 2.2A and C; Control vs. *Mafb*$^{\Delta Endo}$; 3 W, 100 ± 8.3 vs. 30.5 ± 4.4%; 8 W, 100 ± 11.5 vs. 29.4 ± 9.3%; 20 W, 100 ± 6.5 vs. 38.9 ± 4.4%), while the islet architecture and total islet cell number were unaffected (Fig. 2.2D).

To confirm the reduction in insulin and glucagon production, I measured the total insulin and glucagon content in whole pancreata from 3- and 8-week-old animals (Fig. 2.2E and F). Expectedly, the insulin content in the *Mafb*$^{\Delta Endo}$ pancreata was significantly reduced when compared with control pancreata at 3 weeks of age but the insulin content improved to approximately the control levels by 8 weeks of age (Fig. 2.2E; Control vs. *Mafb*$^{\Delta Endo}$; 3 W, 12.8 ± 0.5 vs. 7.6 ± 1.0 ng/μg protein; 8 W, 12.4 ±

0.8 vs. 10.8 ± 0.5 ng/μg protein), which is consistent with the restoration of the Ins^+ cell population (Fig. 2.2B). In contrast, the glucagon content in the *Mafb*$^{\Delta Endo}$ pancreata was severely compromised at both 3 and 8 weeks of age with no sign of recovery to the control levels (Fig. 2.2F; Control vs. *Mafb*$^{\Delta Endo}$; 3 W, 869.7 ± 37.8 vs. 220.8 ± 25.0 pg/μg protein; 8 W, 467.1 ± 30.5 vs. 157.9 ± 16.3 pg/μg protein). Of note, this α-cell abnormality in the *Mafb*$^{\Delta Endo}$ mice did not affect their growth, as the body weight and pancreas weight were both unaltered (Fig. 2.3A and B). Thus, the loss of *Mafb* during embryogenesis affects pancreatic endocrine cell development at early postnatal periods, leading to a decreased population of both Ins^+ and Glu^+ cells. However, only the α-cell defect persists into adulthood because MafB expression becomes restricted to α-cells in mature mice.

Endocrine cell-specific *Mafb* deficiency during the embryonic stage delays insulin production in β-cells and suppresses α-cell development after birth.

MafB is known to regulate not only α- and β-cell differentiation during embryogenesis (11) but also glucagon gene transcription in α-cells (9). Therefore, whether the defect in the α- and β-cell differentiation and/or the suppressed expression of the glucagon gene could cause the drastic decrease in the Ins^+ and Glu^+ cells observed in the *Mafb*$^{\Delta Endo}$ mice remains unknown. To address this question and more precisely investigate the role of MafB in postnatal islet cell development, I performed immunofluorescence staining to examine the expression of β- and α-cell fate markers that characterize cell identity. Pancreas sections from 3- and 8-week-old mice were co-stained for either insulin and Nkx6.1 in β-cells (18) or glucagon and Arx in α-cells (19) (Fig. 2.4A and D). The total $Nkx6.1^+$ cell population remained unchanged, suggesting that the *Mafb* ablation does not affect the β-cell lineage

differentiation (Fig. 2.4A and B; Control vs. *Mafb*$^{\Delta Endo}$; 3 W, 100 ± 8.1 vs. 95.3 ± 9.2%; 8 W, 100 ± 6.8 vs. 106.6 ± 12.0%). At 3 weeks of age, only 60% of the Nkx6.1^{+} cells expressed insulin in the *Mafb*$^{\Delta Endo}$ pancreata, whereas nearly all Nkx6.1^{+} cells from the control pancreata were positive for insulin (Fig. 2.4A and C; Control vs. *Mafb*$^{\Delta Endo}$; 98.4 ± 0.6 vs. 59.2 ± 3.0%). However, the decreased insulin defect was minimized by 8 weeks of age, at which point the Ins^{+} β-cells (Nkx6.1^{+}/Ins^{+}) accounted for more than 90% of the Nkx6.1^{+} cell population (Fig. 2.4A and C; Control vs. *Mafb*$^{\Delta Endo}$; 99.0 ± 0.2 vs. 91.7 ± 1.4%). Thus, embryonic *Mafb* deficiency in pancreatic islets causes delayed insulin production in β-cells without affecting cell fate differentiation. The measurement of the fasting blood glucose levels and glucose metabolism by an intraperitoneal glucose tolerance test further supported my findings of a delayed β-cell development. The *Mafb*$^{\Delta Endo}$ mice showed a higher fasting blood glucose level at P0, which became corrected to the control level by 8 weeks of age (Fig. 2.5A); the delayed glucose tolerance observed in the *Mafb*$^{\Delta Endo}$ mice at 4 weeks of age recovered to the control level by 8 weeks of age (Fig. 2.5B and C).

In contrast, the total Arx^{+} cell population in the *Mafb*$^{\Delta Endo}$ mice was reduced at both time points (Fig. 2.4D and E; Control vs. *Mafb*$^{\Delta Endo}$; 3 W, 100 ± 8.5 vs. 74.1 ± 6.6%; 8 W, 100 ± 9.0 vs. 59.7 ± 3.8%). Similarly, 3-week-old *Mafb*$^{\Delta Endo}$ mice displayed a considerably lower population of Glu^{+} α-cells (Arx^{+}/Glu^{+}), and fewer than 50% of the Arx^{+} cells expressed glucagon (Fig. 2.4D and F; Control vs. *Mafb*$^{\Delta Endo}$; 98.7 ± 0.3 vs. 47.5 ± 3.6%). In contrast to the β-cells, this low population of Glu^{+} α-cells was sustained even at 8 weeks of age without any sign of improvement (Fig. 2.4D and F; Control vs. *Mafb*$^{\Delta Endo}$; 98.0 ± 0.6 vs. 51.4 ± 6.0%). Thus, not only the

reduction of Arx^+ cells but also the diminished expression of glucagon in the Arx^+ cells attributes to the decrease in the Glu^+ cell population in the *Mafb*$^{\Delta Endo}$ mice. Therefore, MafB is required for glucagon production and α-cell lineage development. Interestingly, the remaining Glu^+ α-cells in the *Mafb*$^{\Delta Endo}$ pancreas did not express MafB (Fig. 2.4G), suggesting that an alternative glucagon production pathway independent of MafB exists, which could account for the minimal glucagon content level (Fig. 1F).

2-3. Discussion

This study demonstrates the requirement of MafB in the β-cell terminal differentiation and α-cell development. Only the glucagon production, but not insulin production, showed a persistent defect in the *Mafb*$^{\Delta Endo}$ pancreas with a decreased population of Arx^+ α-cells throughout postnatal development to adulthood. My results from neonates and adult mice expand the previously defined role of MafB in the embryo pancreas. When taken together, MafB plays a significant role in β-cell terminal differentiation and α-cell lineage development including glucagon production but is not required in adult mouse β-cells.

Consistent with previous reports (10, 11), *Mafb* ablation only delayed β-cell development because MafB is not expressed in postnatal rodent β-cells (8, 14). However, my observations in α-cells were inconsistent with a prior study conducted by Conrad *et al.* (10). Pancreas-specific *Mafb* conditional knockout (*Mafb*$^{f/f}$::*Pdx1*-Cre, *Mafb*$^{\Delta panc}$) mice recover Glu^+ α-cells by 2 weeks of age and islet glucagon content by 8 weeks of age (10). This discrepancy may reflect the use of mice with different genetic backgrounds in the present study, whereas the difference in the Cre-drivers

used is unlikely to have contributed because I also generated a *Mafb* conditional knockout mice using *Pdx1*-Cre (20) that exhibited the same phenotype as the $Mafb^{\Delta Endo}$ mice (data not shown). Indeed, the $Mafb^{f/f}$ mice used in the present study (21, 22) and by Conrad *et al.* (10, 23) were generated in mouse ES cells from different genetic backgrounds, e.g., C57BL/6J and 129S4/SvJae, which may explain the phenotypic variations.

Compensation by MafA, another Maf transcription factor, likely explains the limited defect in the $Mafb^{\Delta Endo}$ β-cells because MafA regulates many β-cell key genes first regulated by MafB in adult mice (8). However, unexpectedly, the $Mafb^{\Delta Endo}$ β-cells exhibited residual effects, which were likely caused by delayed β-cell terminal differentiation, with Ins^{+} cell populations and insulin content, both minimally but consistently reduced (Fig. 2.2B and E). These results potentially highlight the supporting role played by MafB in postnatal β-cell development. A recent study by van der Meulen *et al*. introduced the novel concept of a "virgin β-cell" subpopulation, which contains functionally immature β-cells characterized as Ins^{+}/$MafB^{+}$/Ucn^{-} (24). This very minor virgin β-cell subpopulation can transdifferentiate into functional β-cells and is found in both mouse and human islets (24). Therefore, they concluded that MafB-expressing virgin β-cells may be the source of β-cell regeneration through trans-differentiation in adult islets (24). Moreover, another study performed by Cheng *et al.* demonstrated that β-cells regenerate from a novel mesenchymal cell population after a near-total ablation of pre-existing β-cells by a high dose of STZ in adult rodents (25). Interestingly, these newly formed β-cells express MafB and vimentin but not Pdx1 and Nkx6.1 and are, thus, immature. However, these cells gradually acquire functional maturity and became bona fide β-cells (25). These findings suggest

that β-cell regeneration is preceded by MafB expression in β-cells, which is lost upon functional maturity. Thus, the role of MafB in the facilitation of β-cell development cannot be neglected.

2-4. Materials and Methods

Animals

Mice were maintained under specific pathogen-free conditions at the Laboratory Animal Resource Center of the University of Tsukuba. All animal experiments were approved by the Institutional Animal Care and Use Committee of the University of Tsukuba. To investigate endocrine cell-specific emission of tdsRed, ROSA26 knock-in Cre-reporter C57BL/6N (R25GRR) mice (17) were crossed with *Neurogenin3* (*Ngn3*)-Cre transgenic mice (16) to obtain R26GRR::Ngn3-Cre F_1 progeny. The endocrine cell-specific *Mafb* knockout mice were generated by crossing $Mafb^{f/f}$ mice (21, 22) with *Ngn3*-Cre mice (16). The $Mafb^{f/f}$ mice were generated on a C57BL/6J strain background as previously described (21, 22). The *Ngn3*-Cre transgenic mouse strain was kindly provided by Dr. Shosei Yoshida (Division of Germ Cell Biology, National Institute for Basic Biology, JAPAN). In this study, $Mafb^{f/f}$::*Ngn3*-Cre is referred to as $Mafb^{\Delta Endo}$ mice. The $Mafb^{f/f}$ littermates were used as controls.

Validation of Cre recombination

The pancreatic tissues were fixed for 4 h in 4% paraformaldehyde (PFA) in phosphate-buffered saline (PBS) at 4°C, transferred to 30% sucrose solution overnight, and embedded in OCT compounds (Tissue-Tek, Sakura Fietek) before being frozen. Then, 5-μm sections were sliced and mounted with Fluoromount

(Diagnostic BioSystems). All images were acquired under a fluorescence microscope (BIOREVO BZ-9000, Keyence).

Immunohistochemistry

The pancreatic tissues were fixed overnight in 4% PFA in PBS at 4°C, processed, and embedded in paraffin. Then, 2-μm sections were sliced and prepared according to standard methods. For the nuclear protein staining, the sections were soaked in 0.3% Triton X-100/PBS solution, followed by heat-induced epitope retrieval using Target Retrieval Solution (Dako) and a pressure cooker. All sections were blocked with appropriate serum for 1 h at room temperature and incubated overnight at 4°C with the following primary antibodies: guinea pig anti-insulin (1:500; ab7842, Abcam), rabbit anti-glucagon (1:2000; 2760, Cell Signaling), guinea pig anti-glucagon (1:1000; M182, Takara), rabbit anti-Arx (1:250; generous gift from Drs. Kunio Kitamura and Ken-ichirou Morohashi, Kyushu University, JAPAN) (26), mouse anti-Nkx6.1 (1:250; F55A10, DSHB) and rabbit anti-MafB (1:100; IHC-00351, Bethyl). The antigens were visualized using appropriate secondary antibodies conjugated to Alexa Flour 488 or 594 (1:1000; Life Technologies), and the nuclei were labeled with Hoechst 33342 (Molecular Probes). The tissue specimens were mounted with Fluoromount (Diagnostic BioSystems). All images were acquired under a fluorescence microscope (BIOREVO BZ-9000, Keyence).

Cell counting

Following the immunofluorescence staining, the numbers of different cell types in the islet microscopy images of each islet were manually counted. For each cell type, 20-40 representative islets from 3-6 mice per group were counted. To calculate the

fraction of Ins^+ and Glu^+ cells within the islets, the number of Ins^+ or Glu^+ cells per islet was manually counted using ImageJ software and divided by the total number of $Hoechst^+$ nuclei from the same islet (% $hormone^+$ cells/islet $Hoechst^+$ nuclei) and then normalized to the control group. The fractions of $Nkx6.1^+/Ins^+$ and Arx^+/Glu^+ cells were determined by dividing the number of double-positive cells per islet by the total numbers of $Nkx6.1^+$ ($Nkx6.1^+/Ins^-$ and $Nkx6.1^+/Ins^+$) and Arx^+ (Arx^+/Glu^- and Arx^+/Glu^+) cells, respectively. The total $Nkx6.1^+$ and Arx^+ cell counts were normalized to their corresponding controls.

Measurement of pancreatic insulin and glucagon content

The whole pancreas was collected from 3- and 8-week-old *Mafb*$^{\Delta Endo}$ mice and homogenized in ice-cold acetic-ethanol buffer (1.5% HCl in 75% ethanol) as previously described (27). The total insulin and glucagon contents in the pancreatic tissue extracts were measured via enzyme-linked immunosorbent assay (ELISA) according to the manufacturer's instructions (Morinaga Mouse Insulin ELISA Kit, M1102; Mercodia Glucagon 10 µl ELISA Kit, 10-1281-01). Each pancreatic content was normalized according to the total protein concentration per sample, which was determined using Bradford reagent (Thermo Fisher Scientific).

Intraperitoneal glucose tolerance test (ipGTT)

Four- and 8-week-old *Mafb*$^{\Delta Endo}$ male mice and their corresponding controls were fasted for 16 h overnight. On the following morning, 2 mg/g body weight of glucose (Otsuka) was injected intraperitoneally, and the blood glucose level was measured from the tail blood using a glucometer (Terumo, GR-101) 0, 15, 30, 60, and 120 min post-injection.

Statistical analysis

All data are presented as the mean ± SEM. To determine the statistical significance between the MafB mutants and controls, a minimum of three biological replicates were analyzed by performing Welch's *t*-test, and a p-value < 0.05 was considered significant. To compare the longitudinal data obtained from the ipGTT, the *p*-values were calculated by performing Welch's *t*-test, followed by Holm's correction for multiple comparisons.

2-5. Figures and Legends

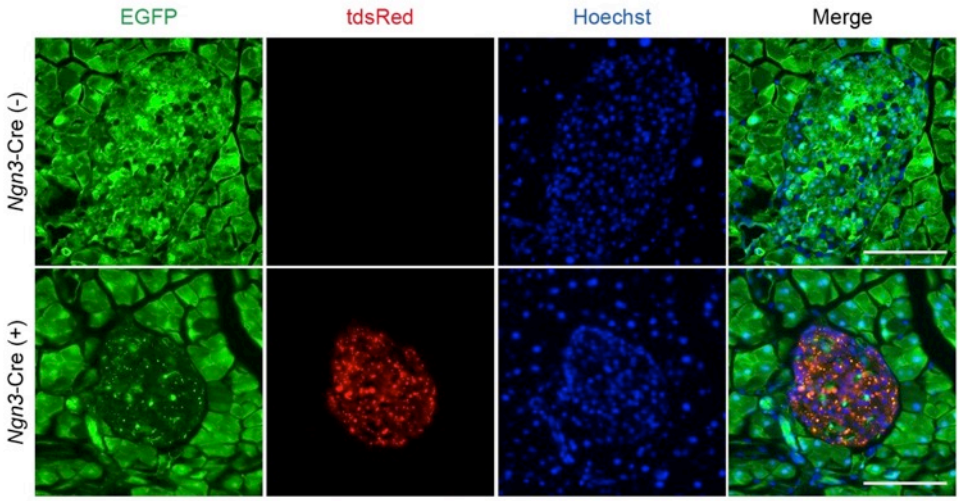

Fig. 2.1 *Ngn3*-Cre driver expresses Cre recombinase in pancreatic endocrine cells.

EGFP (non-Cre-recombined cells) and tdsRed (Cre-recombined cells) expression in the pancreas of R26GRR::*Ngn3*-Cre and control (R26GRR) mice at 3 weeks of age. Nuclei were stained with Hoechst 33342. Scale bars, 50 μm.

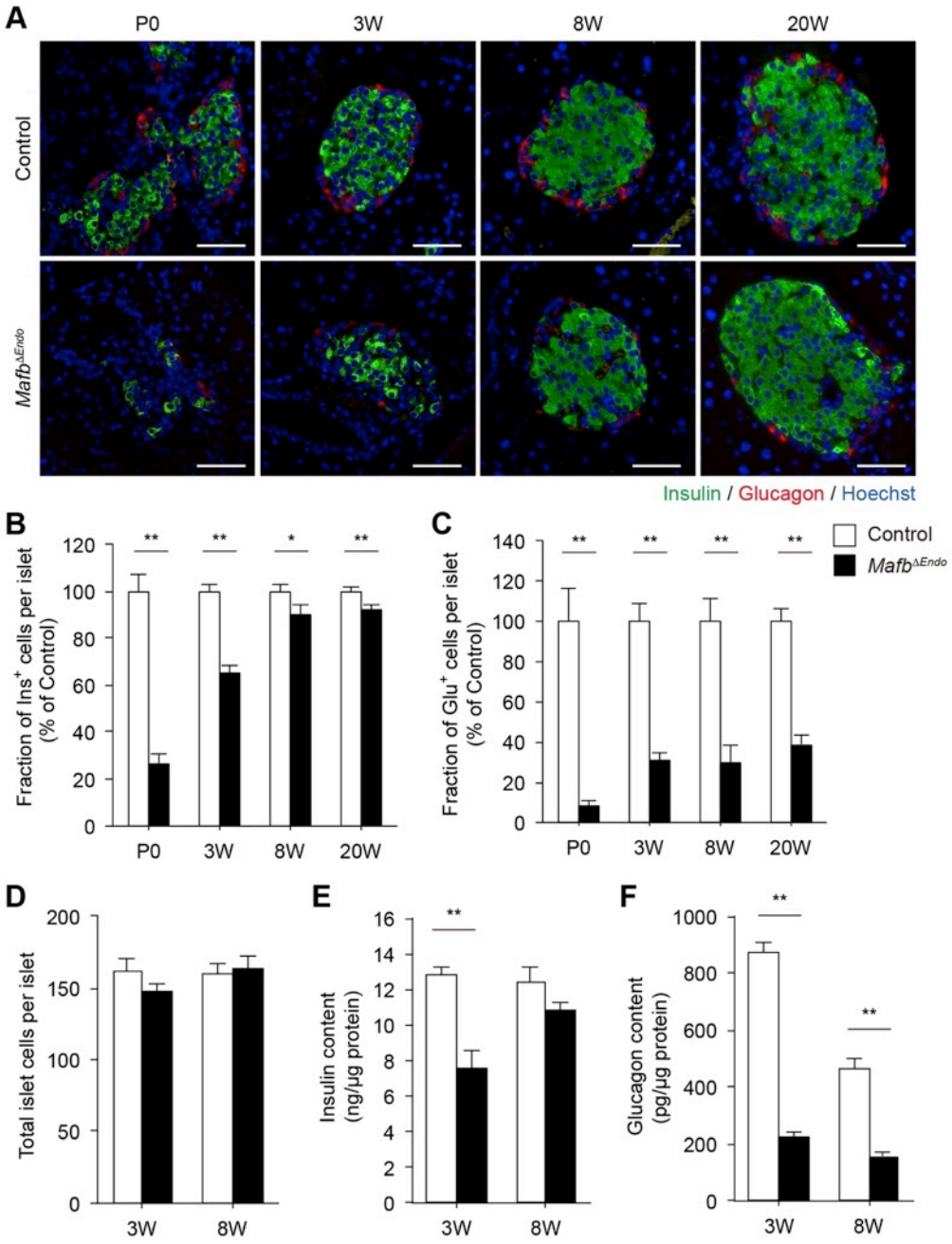

Fig. 2.2 Embryonic deletion of *Mafb* in endocrine cells decreases the population of both Ins^+ and Glu^+ cells postnatally.

Fig. 2.2 Embryonic deletion of *Mafb* in endocrine cells decreases the population of both Ins^+ and Glu^+ cells postnatally.

(A) Immunostaining of insulin (green) and glucagon (red) in $Mafb^{\Delta Endo}$ and control ($Mafb^{f/f}$) pancreata from P0 and 3-, 8-, and 20-week-old animals. Nuclei were stained with Hoechst 33342. Scale bars, 50 μm. **(B)** Fraction of Ins^+ and **(C)** Glu^+ cells within the islets in $Mafb^{\Delta Endo}$ (closed bars) and control (open bars) pancreata ($n \geq 3$). All values were normalized to those in age-matched controls. ** $p < 0.01$. (D) Total islet cell number per islet in $Mafb^{\Delta Endo}$ (closed bars) and control (open bars) pancreata from 3- and 8-week-old animals ($n \geq 3$). **(E)** Pancreatic insulin and **(F)** glucagon content in $Mafb^{\Delta Endo}$ (closed bars) and control (open bars) pancreata from 3- and 8-week-old animals ($n \geq 4$). Hormone contents were normalized to the total protein concentration. ** $p < 0.01$.

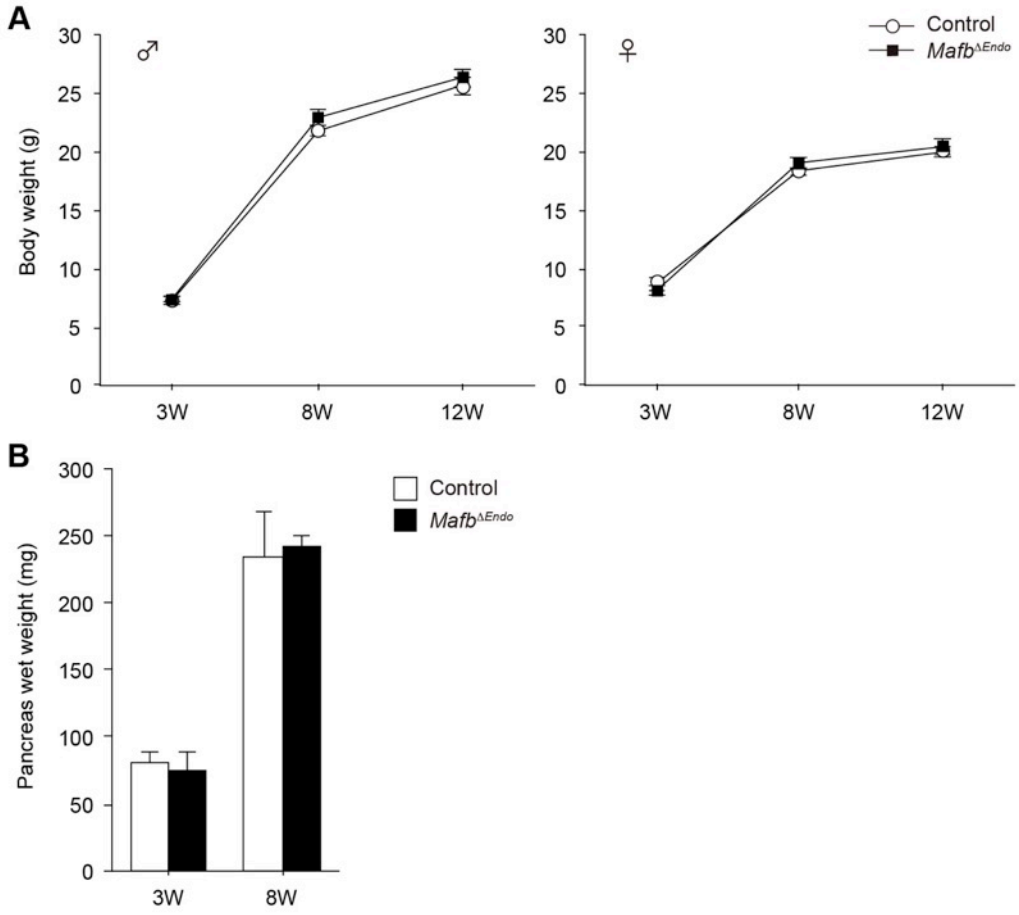

Fig. 2.3. *Mafb*$^{\Delta Endo}$ mice show normal body growth.

(A) Body weight changes in *Mafb*$^{\Delta Endo}$ (closed markers) and control (open markers) animals at 3, 8 and 12 weeks of age ($n \geq 4$). Males are shown on the left and females are shown on the right. **(B)** Pancreas wet weight in *Mafb*$^{\Delta Endo}$ (closed bars) and control (*Mafb*$^{f/f}$, open bars) pancreata from 3- and 8-week-old animals ($n \geq 4$).

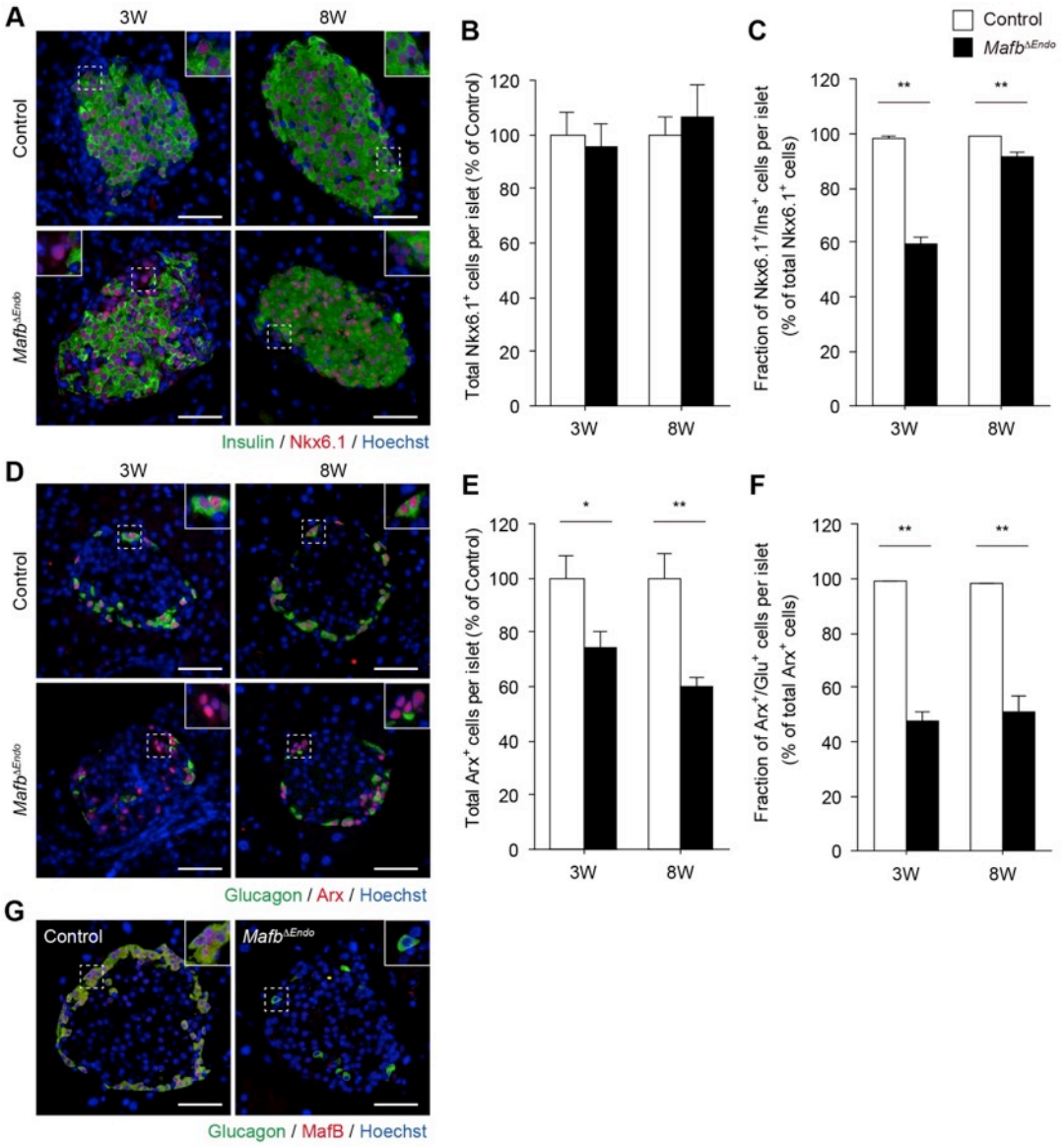

Fig. 2.4 Endocrine cell-specific *Mafb* deficiency during the embryonic stage delays insulin production in β-cells and suppresses α-cell development after birth.

Fig. 2.4 Endocrine cell-specific *Mafb* deficiency during the embryonic stage delays insulin production in β-cells and suppresses α-cell development after birth.

(A) Insulin (green) and Nkx6.1 (red) immunoreactivity in $Mafb^{\Delta Endo}$ and control ($Mafb^{f/f}$) pancreata from 3- and 8-week-old animals. Nuclei were stained with Hoechst 33342. Scale bars, 50 μm. **(B)** Total $Nkx6.1^+$ cells per islets, normalized to those in age-matched controls ($n \geq 4$). **(C)** Fraction of Ins^+ β-cells among the total $Nkx6.1^+$ cell population in $Mafb^{\Delta Endo}$ (closed bars) and control (open bars) pancreata ($n \geq 4$). ** $p < 0.01$. **(D)** Immunofluorescence of glucagon (green) and Arx (red) in $Mafb^{\Delta Endo}$ and control pancreata from 3- and 8-week-old animals. Nuclei were stained with Hoechst 33342. Scale bars, 50 μm. **(E)** Total Arx^+ cells per islets normalized to those in age-matched controls ($n \geq 4$). * $p < 0.05$ and ** $p < 0.01$. **(F)** Fraction of Glu^+ α-cells among the total Arx^+ cell population in $Mafb^{\Delta Endo}$ (closed bars) and control (open bars) pancreata ($n \geq 4$). ** $p < 0.01$. **(G)** Co-staining of glucagon (green) and MafB (red) in 8-week-old $Mafb^{\Delta Endo}$ and control mice. Nuclei were stained with Hoechst 33342. Scale bars, 50 μm.

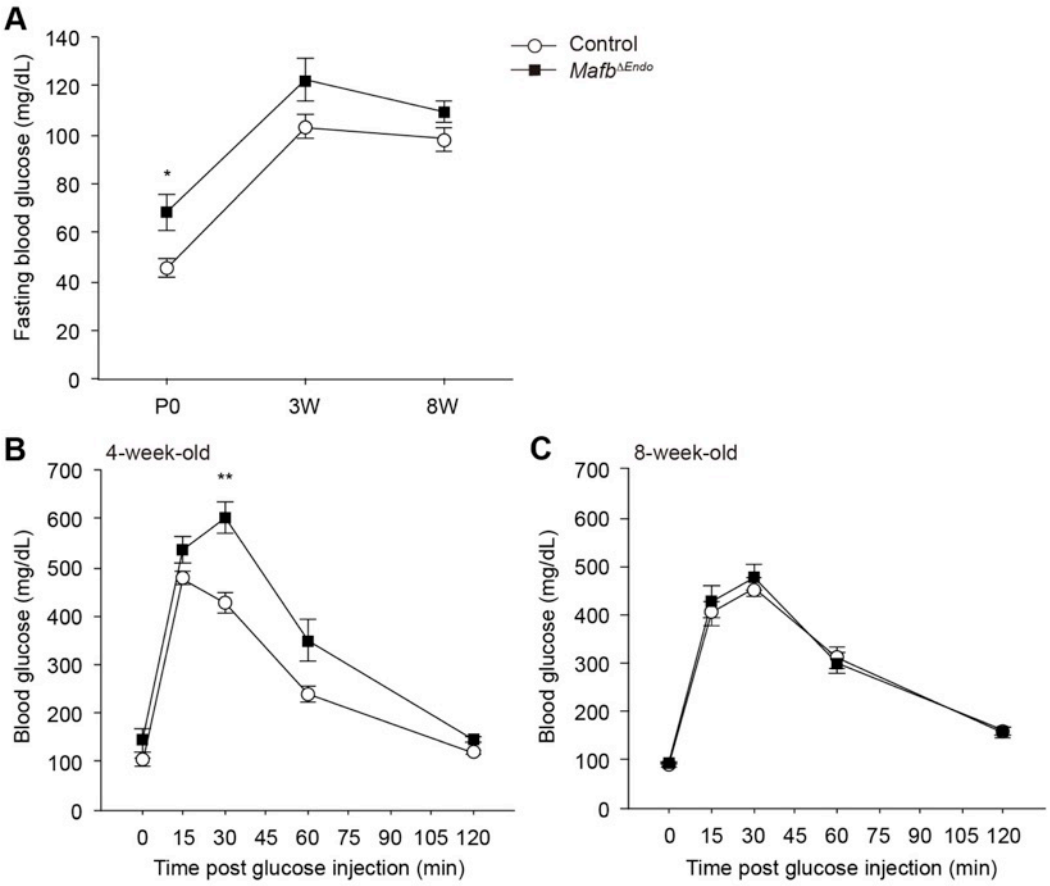

Fig. 2.5 Embryonic loss of *Mafb* in the endocrine cells delays β-cell functional maturation.

(A) Fasting blood glucose measurements in $Mafb^{\Delta Endo}$ (closed markers) and control ($Mafb^{f/f}$, open markers) male mice at P0, 3 and 8 weeks of age ($n \geq 7$). * $p < 0.05$. **(B and C)** Glucose tolerance test after an intraperitoneal injection of glucose (2 mg/g body weight) in $Mafb^{\Delta Endo}$ (closed markers) and control (open markers) male mice at 4 and 8 weeks of age ($n \geq 6$). ** $p < 0.01$.

CHAPTER 3:

The role of MafB in mature α- and β-cells

3-1. Purpose

Although the *in vitro* study demonstrated that MafB is a transcriptional activator of the glucagon gene (9), whether MafB substantially controls glucagon expression in α-cells *in vivo* is unclear. In contrast to Conrad et al.'s report (10), my results from Chapter 2 show that MafB is required for glucagon expression even in adult α-cells *in vivo*. However, I cannot rule out that the possibility that the reduced Arx^{+} cell population, rather than the loss of MafB-activated glucagon gene transcription, disturbs glucagon production in $Mafb^{\Delta Endo}$ α-cells. To remove the effect from abnormal α-cell differentiation caused by the *Mafb* deficiency, I generated another conditional *Mafb* knockout mouse model ($Mafb^{\Delta TAM}$) in which *Mafb* was deleted in adult mice by using the tamoxifen (TAM)-inducible system.

3-2. Results

Loss of *Mafb* in adult mice impairs glucagon expression in mature α-cells without affecting α-cell identity.

To verify the effects of *Mafb* ablation on glucagon production, I generated conditional *Mafb* knockout ($Mafb^{f/f}$::*CAGG*-$CreER^{TM}$, $Mafb^{\Delta TAM}$) mice after pancreatic islet cell maturation by TAM injection at 5 weeks of age. The Cre recombination was detectable in the whole pancreas of R26GRR::*CAGG*-$CreER^{TM}$ mice 3 weeks post-TAM injection which suggest successful TAM-induced Cre recombination (Fig. 3.1). Immunohistochemical examination revealed no significant changes in the organization of the Ins^{+} and Glu^{+} cells in the $Mafb^{\Delta TAM}$ islets compared with that in the $Mafb^{f/f}$ control islets (Fig. 3.2A). Consistent with the undetectable MafB expression in the adult β-cells (8, 14), I did not observe any differences in the Ins^{+} cell population from the control mice (Fig. 3.2A and B; Control

vs. *Mafb*$^{\Delta TAM}$; 3 W post-TAM, 100 ± 2.6 vs. 96.2 ± 2.5%; 11 W post-TAM, 100 ± 1.8 vs. 95.1 ± 2.9%), and thus, no differences were observed in the fasting blood glucose and plasma insulin levels (Fig. 3.3A and B). In contrast, the percentage of Glu^{+} cells in the *Mafb*$^{\Delta TAM}$ islets was drastically reduced at 3 weeks post-TAM injection and further reduced by 11 weeks post-injection (Fig. 3.2A and C; Control vs. *Mafb*$^{\Delta TAM}$; 3 W post-TAM, 100 ± 6.6 vs. 73.3 ± 6.0%; 11 W post-TAM, 100 ± 6.0 vs. 40.0 ± 4.7%). Additionally, expectedly, the insulin content levels were not altered by the *Mafb* deletion in the TAM-injected *Mafb*$^{\Delta TAM}$ pancreata 3 weeks post-injection (Fig. 3.2D; Control vs. *Mafb*$^{\Delta TAM}$; 11.2 ± 0.4 vs. 13.0 ± 0.9 ng/μg protein), whereas the glucagon levels were approximately 65% of the control levels (Fig. 3.2E; Control vs. *Mafb*$^{\Delta TAM}$; 437.3 ± 18.6 vs. 283.8 ± 17.6 pg/μg protein). Taken together, these results indicate that *Mafb* deficiency in adult mice alters hormone expression in α-cells but not β-cells, demonstrating that sustained MafB function is required for normal glucagon production by α-cells from postnatal development to maturity.

I further investigated whether the *Mafb* ablation in the adult mice influenced the islet cell identity. At 3 and 11 weeks post-TAM injection, the total Nkx6.1^{+} cell population in the *Mafb*$^{\Delta TAM}$ pancreata did not differ from that in the controls (Fig. 3.4A and B; Control vs. *Mafb*$^{\Delta TAM}$; 3 W post-TAM, 100 ± 10.9 vs. 104.5 ± 7.9%; 11 W post-TAM, 100 ± 8.4 vs. 96.4 ± 5.7%). In addition, nearly all Nkx6.1^{+} cells expressed insulin, albeit a slightly lower level in *Mafb*$^{\Delta TAM}$ pancreata when compared with the controls (Fig. 3.4A and C; Control vs. *Mafb*$^{\Delta TAM}$; 3 W post-TAM, 98.8 ± 0.4 vs. 97.2 ± 0.5%; 11 W post-TAM, 98.4 ± 0.4 vs. 96.4 ± 0.5%). Thus, MafB does not significantly affect mature β-cells. In contrast, while the total Arx^{+} cell population was similar to that in the controls (Fig. 3.4D and E; Control vs. *Mafb*$^{\Delta TAM}$; 3 W post-

TAM, 100 ± 13.1 vs. 98.1 ± 7.4%; 11 W post-TAM, 100 ± 8.1 vs. 98.4 ± 6.6%), a marked decrease in the Glu^+ α-cell population was observed (Fig. 3.4D and F; Control vs. $Mafb^{\Delta TAM}$; 3 W post-TAM, 98.6 ± 0.4 vs. 68.8 ± 4.4%; 11 W post-TAM, 99.4 ± 0.3 vs. 58.3 ± 4.1%). The reduced proportion of Glu^+ α-cells is not caused by α-cell apoptosis as confirmed by negative signals in the TUNEL assay (Fig. 3.5A). Furthermore, the total islet cell number in the $Mafb^{\Delta TAM}$ pancreata remained unchanged (Fig. 3.5B), which is similar to that observed in the $Mafb^{\Delta Endo}$ mice (Fig. 2.2D). However, a minimum level of glucagon expression was observed even in the absence of MafB in the $Mafb^{\Delta TAM}$ pancreata (Fig. 3.4G), which is consistent with that observed in the $Mafb^{\Delta Endo}$ mice and suggests that a MafB independent pathway of glucagon production exists. Overall, my results indicate that MafB is critical for the maintenance of α-cell function in adult mice, confirming the principal role of MafB in glucagon expression.

3-3. Discussion

This study demonstrates the decisive role of MafB in the maintenance of α-cell function by controlling glucagon production. The *Mafb* deletion after islet maturation reduced glucagon production without defecting the expression of α-cell fate marker and did not show a significant effect on mature β-cells. These findings strongly support my conclusion that MafB is crucial for glucagon production in α-cells.

In contrast to mice, MAFB expression in human β-cells is retained postnatally (14, 28), thereby implicating human MAFB in β-cell maintenance and/or activity. Notably, severe reductions in MAFB levels are observed in human type 2 diabetic islets, suggesting that β-cell failure is associated with low MAFB expression (29). In

addition, *in vitro* studies using a human β-cell line (EndoC-βH1) demonstrated that MAFB is required for glucose-stimulated insulin secretion in human β-cells, indicating that mature human β-cells require MAFB for their functional activity (30). However, clinical reports of patients carrying MAFB mutations do not include the blood glucose levels or HbA1c status (31–33), leading to the impression that these patients are normoglycemic. Further investigations are required to clarify the role of MAFB in human β-cells.

3-4. Materials and Methods

Animals

Mice were maintained under specific pathogen-free conditions at the Laboratory Animal Resource Center of the University of Tsukuba. All animal experiments were approved by the Institutional Animal Care and Use Committee of the University of Tsukuba. To investigate tamoxifen-mediated emission of tdsRed, ROSA26 knock-in Cre-reporter C57BL/6N (R25GRR) mice (17) were crossed with *CAGG*-CreER^{TM} transgenic mice (JAX stock number 004682) (34) to obtain R26GRR::*CAGG*-CreER^{TM} F_1 progeny. Tamoxifen (TAM)-dependent *Mafb* knockout mice were generated by crossing *Mafb*$^{f/f}$ mice (21, 22) with *CAGG*-CreER^{TM} transgenic mice (JAX stock number 004682) (34). The *Mafb*$^{f/f}$ mice were generated on a C57BL/6J strain background as previously described (21, 22). In this study, *Mafb*$^{f/f}$::*CAGG*-CreER^{TM} is referred to as *Mafb*$^{\Delta TAM}$ mice. The *Mafb*$^{f/f}$ littermates were used as controls. To activate the Cre recombination system in the *CAGG*-CreER^{TM} strain, 5-week-old *Mafb*$^{\Delta TAM}$ and their control groups were injected intraperitoneally with 75 mg/kg body weight of TAM for 5 consecutive days (35). TAM (Sigma) was first dissolved in ethanol and then mixed with corn oil as described previously (36).

Validation of Cre recombination

The pancreatic tissues were fixed for 4 h in 4% paraformaldehyde (PFA) in phosphate-buffered saline (PBS) at 4°C, transferred to 30% sucrose solution overnight, and embedded in OCT compounds (Tissue-Tek, Sakura Fietek) before being frozen. Then, 5-μm sections were sliced and mounted with Fluoromount (Diagnostic BioSystems). All images were acquired under a fluorescence microscope (BIOREVO BZ-9000, Keyence).

Immunohistochemistry

The pancreatic tissues were fixed overnight in 4% paraformaldehyde (PFA) in phosphate-buffered saline (PBS) at 4°C, processed, and embedded in paraffin. Then, 2-μm sections were sliced and prepared according to standard methods. For the nuclear protein staining, the sections were soaked in 0.3% Triton X-100/PBS solution, followed by heat-induced epitope retrieval using Target Retrieval Solution (Dako) and a pressure cooker. All sections were blocked with appropriate serum for 1 h at room temperature and incubated overnight at 4°C with the following primary antibodies: guinea pig anti-insulin (1:500; ab7842, Abcam), rabbit anti-glucagon (1:2000; 2760, Cell Signaling), guinea pig anti-glucagon (1:1000; M182, Takara), rabbit anti-Arx (1:250; generous gift from Drs. Kunio Kitamura and Ken-ichirou Morohashi, Kyushu University, JAPAN) (26), mouse anti-Nkx6.1 (1:250; F55A10, DSHB) and rabbit anti-MafB (1:100; IHC-00351, Bethyl). The antigens were visualized using appropriate secondary antibodies conjugated to Alexa Flour 488 or 594 (1:1000; Life Technologies), and the nuclei were labeled with Hoechst 33342 (Molecular Probes). The tissue specimens were mounted with Fluoromount

(Diagnostic BioSystems). All images were acquired under a fluorescence microscope (BIOREVO BZ-9000, Keyence).

Cell counting

Following the immunofluorescence staining, the numbers of different cell types in the islet microscopy images of each islet were manually counted. For each cell type, 20-40 representative islets from 3-6 mice per group were counted. To calculate the fraction of Ins^+ and Glu^+ cells within the islets, the number of Ins^+ or Glu^+ cells per islet was manually counted using ImageJ software and divided by the total number of $Hoechst^+$ nuclei from the same islet (% $hormone^+$ cells/islet $Hoechst^+$ nuclei) and then normalized to the control group. The fractions of $Nkx6.1^+/Ins^+$ and Arx^+/Glu^+ cells were determined by dividing the number of double-positive cells per islet by the total numbers of $Nkx6.1^+$ ($Nkx6.1^+/Ins^-$ and $Nkx6.1^+/Ins^+$) and Arx^+ (Arx^+/Glu^- and Arx^+/Glu^+) cells, respectively. The total $Nkx6.1^+$ and Arx^+ cell counts were normalized to their corresponding controls.

Measurement of pancreatic insulin and glucagon content

The whole pancreas was collected from $Mafb^{\Delta TAM}$ mice 3 weeks post-TAM injection and homogenized in ice-cold acetic-ethanol buffer (1.5% HCl in 75% ethanol) as previously described (27). The total insulin and glucagon contents in the pancreatic tissue extracts were measured via enzyme-linked immunosorbent assay (ELISA) according to the manufacturer's instructions (Morinaga Mouse Insulin ELISA Kit, M1102; Mercodia Glucagon 10 μl ELISA Kit, 10-1281-01). Each pancreatic content was normalized according to the total protein concentration per sample, which was determined using Bradford reagent (Thermo Fisher Scientific).

Measurement of blood glucose and plasma insulin concentration

The blood glucose and plasma insulin levels were measured after an 16h overnight fasting. On the following morning, the blood glucose level was measured from the tail blood using a glucometer (Terumo, GR-101). To determine the plasma insulin level, venous blood was collected into a heparinized tube (Drummond Scientific Company) and assayed using the Morinaga Mouse Insulin ELISA Kit (M1102).

TUNEL staining

Apoptotic cells in paraffin-embedded pancreas sections were detected using the TUNEL labeling method on a DeadEnd^{TM} Fluorometric TUNEL system (Promega) according to the manufacturer's instructions. Positive control slides were prepared by performing an additional step of DNase-1 treatment to induce DNA fragmentation. Nuclei were counter-stained with Hoechst 33342 (Molecular Probes) before the analysis under a fluorescence microscope (BIOREVO BZ-9000, Keyence).

Statistical analysis

All data are presented as the mean ± SEM. To determine the statistical significance between the MafB mutants and controls, a minimum of three biological replicates were analyzed by performing Welch's *t*-test, and a p-value < 0.05 was considered significant.

3-5. Figures and Legends

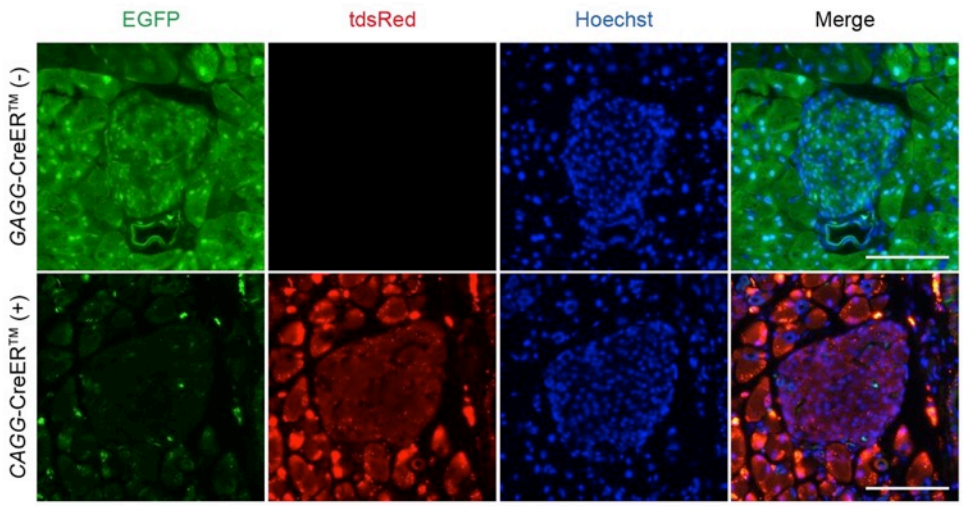

Fig. 3.1 Cre recombination in *CAGG*-CreER^{TM} driver is activated by tamoxifen.

EGFP (non-Cre-recombined cells) and tdsRed (Cre-recombined cells) expression in the pancreas of R26GRR::*CAGG*-CreER^{TM} and control (R26GRR) mice 3 weeks post-tamoxifen (TAM) injection. TAM was injected at 5 weeks of age. Nuclei were stained with Hoechst 33342. Scale bars, 50 μm.

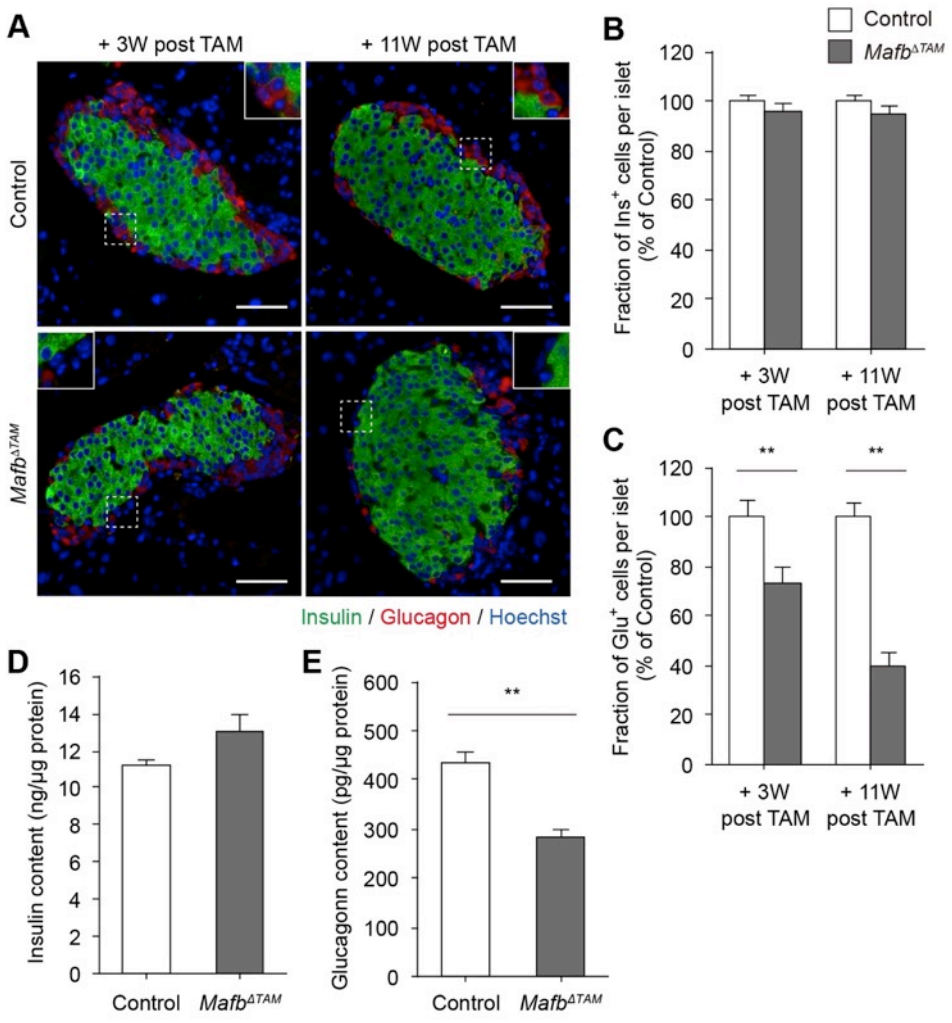

Fig. 3.2 Loss of *Mafb* in adult mice impairs glucagon expression in mature α-cells.

Fig. 3.2 Loss of *Mafb* in adult mice impairs glucagon expression in mature α-cells. **(A)** Immunostaining of insulin (green) and glucagon (red) in $Mafb^{\Delta TAM}$ and control ($Mafb^{f/f}$) pancreata from mice 3 and 11 weeks post-tamoxifen (TAM) injection. TAM was injected at 5 weeks of age. Nuclei were stained with Hoechst 33342. Scale bars, 50 μm. **(B)** Fraction of Ins^+ and **(C)** Glu^+ cells among islets in $Mafb^{\Delta TAM}$ (closed bars) and control (open bars) pancreata ($n \geq 4$). All values were normalized to those in age-matched controls. ** $p < 0.01$. **(D)** Pancreatic insulin and **(E)** glucagon content in $Mafb^{\Delta TAM}$ (closed bars) and control (open bars) pancreata from mice 3 weeks post-TAM injection ($n = 6$). Hormone contents were normalized to the total protein concentration. ** $p < 0.01$.

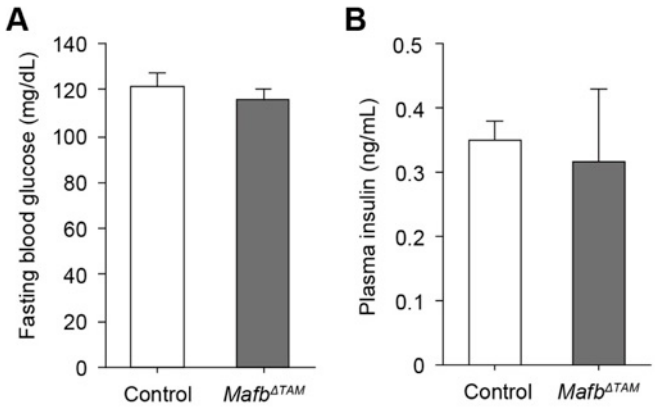

Fig. 3.3 *Mafb*$^{\Delta TAM}$ mice show normal fasting blood glucose and plasma insulin levels. **(A)** Fasting blood glucose level ($n \geq 7$) and **(B)** plasma insulin concentration ($n = 4$) in *Mafb*$^{\Delta TAM}$ (closed bars) and control (*Mafb*$^{f/f}$, open bars) male mice at 11 weeks post-tamoxifen (TAM) injection. TAM was injected at 5 weeks of age.

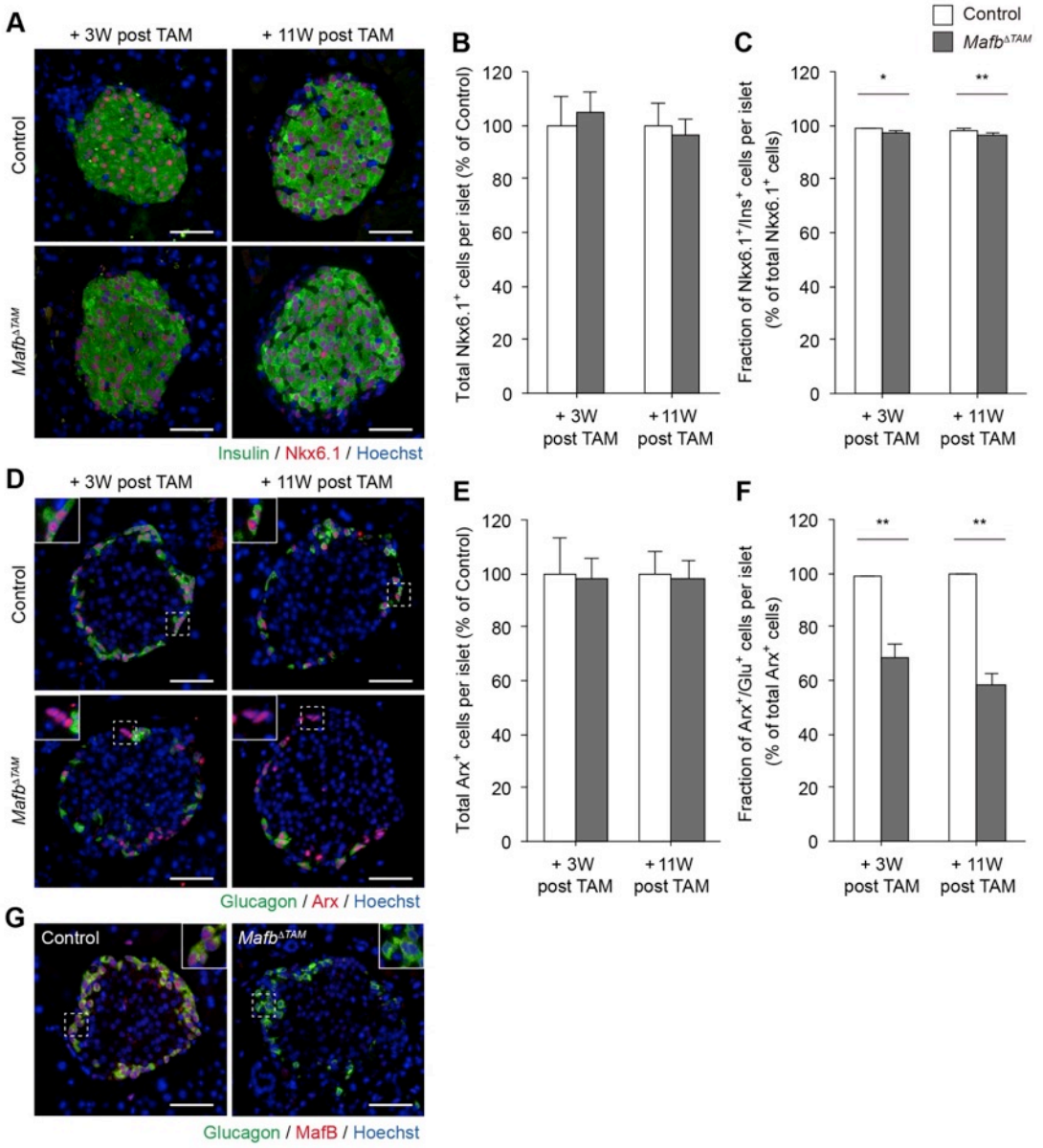

Fig. 3.4 Adult-onset ablation of *Mafb* does not affect α-cell identity but suppresses glucagon expression.

Fig. 3.4 Adult-onset ablation of *Mafb* does not affect α-cell identity but suppresses glucagon expression.

(A) Insulin (green) and Nkx6.1 (red) immunoreactivity in $Mafb^{\Delta TAM}$ and control ($Mafb^{f/f}$) pancreata from mice 3 and 11 weeks post-tamoxifen (TAM) injection. TAM was injected at 5 weeks of age. Nuclei were stained with Hoechst 33342. Scale bars, 50 μm. **(B)** Total $Nkx6.1^+$ cells per islets normalized to those in age-matched controls ($n \geq 4$). **(C)** Fraction of Ins^+ β-cells among the total $Nkx6.1^+$ cell population in $Mafb^{\Delta TAM}$ (closed bars) and control (open bars) pancreata ($n \geq 4$). * $p < 0.05$ and ** $p < 0.01$. **(D)** Immunofluorescence of glucagon (green) and Arx (red) in $Mafb^{\Delta TAM}$ and control pancreata from mice 3 and 11 weeks post-TAM injection. Nuclei were stained with Hoechst 33342. Scale bars, 50 μm. **(E)** Total Arx^+ cells per islets normalized to those in age-matched controls ($n \geq 4$). **(F)** Fraction of Glu^+ α-cells among the total Arx^+ cell population in $Mafb^{\Delta TAM}$ (closed bars) and control (open bars) pancreata ($n \geq 4$). ** $p < 0.01$. **(G)** Co-staining of glucagon (green) and MafB (red) 3 weeks post-TAM injection in $Mafb^{\Delta TAM}$ and control mice. Nuclei were stained with Hoechst 33342. Scale bars, 50 μm.

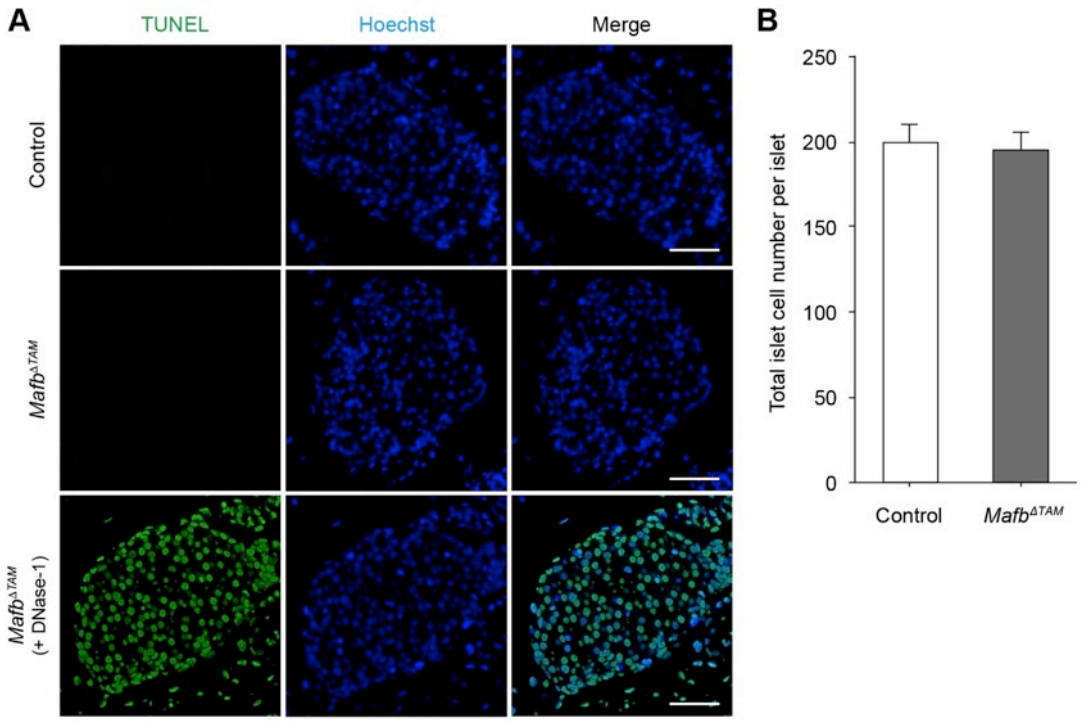

Fig. 3.5 Tamoxifen-induced *Mafb* deletion does not affect islet cell viability.

(A) Detection of apoptosis by TUNEL assay in *Mafb*$^{\Delta TAM}$ and control (*Mafb*$^{f/f}$) pancreata from mice 11 weeks post-tamoxifen (TAM) injection. TAM was injected at 5 weeks of age. Positive control slides (bottom panels) were treated with DNase-1 before the TdT reaction. Nuclei were stained with Hoechst 33342. Scale bars, 50 μm. **(B)** Total islet cell number per islet in *Mafb*$^{\Delta TAM}$ (closed bars) and control (open bars) pancreata from mice 11 weeks post-TAM injection ($n \geq 4$).

CHAPTER 4:

The role of MafB in islet cell lineage commitment

4-1. Purpose

Because MafB affects both of α- and β-cell development, whose precursors are shared by PP- and δ-cells, respectively, I examined MafB's involvement in other islet cell types.

4-2. Results

MafB expression during embryonic development favors α-cell lineage commitment by suppressing PP-cell differentiation.

First, I performed immunostaining of somatostatin (Som)-producing δ-cells and pancreatic polypeptide (PP)-producing PP-cells to identify any changes in these cell populations (Fig. 4.1A and C). In both 3- and 8-week-old *Mafb*$^{\Delta Endo}$ pancreas, the Som^{+} cell population remained unaffected (Fig. 4.1A and B). However, the PP^{+} cell population increased by approximately 3.5-fold compared with that in the controls at both ages (Fig. 4.1C and D; Control vs. *Mafb*$^{\Delta Endo}$; 3 W, 100 ± 16.6 vs. 387.7 ± 45.9%; 8 W, 100 ± 26.4 vs. 352.1 ± 39.2%). Because PP-cells share a common precursor with α-cells, I investigated whether the increased PP^{+} cell population originates from a cell fate change induced by the *Mafb* deletion in α-cells; I conducted immunohistochemistry by co-staining using glucagon/PP or Arx/PP antibodies (Fig. 4.1E and F). Surprisingly, most PP expression did not merge with the glucagon signal (Fig. 4.1E) but consistently merged with the Arx expression regardless of the genotype (Fig. 4.1F), suggesting that PP^{+} cells mainly originate from Arx^{+}/Glu^{-} cells. Although PP^{+}/Glu^{+} double positive cells were rarely observed as previously reported (37), this subpopulation remained unaltered in both groups, excluded from the cell source of the Arx^{+}/PP^{+} cell population. More strikingly, the significant 3.5-fold increase in the PP^{+} cell population was equivalent to the decreased fold change in the

Glu^+ cell fraction (Fig. 4.1D and 2.2C), suggesting that the diminished glucagon-producing cell population could be compensated for by the increased PP-producing cell population. These differences (approximately 3.5-fold change) were consistently observed in both the 3- and 8-week-old *Mafb*$^{\Delta Endo}$ mice (Fig. 4.1D); whereas, the *Mafb*$^{\Delta TAM}$ mice did not exhibit any change in any cell type population, including the δ- and PP-cell populations (Fig. 4.2A and B; Control vs. *Mafb*$^{\Delta TAM}$; Som^+, 100 ± 9.2 vs. 118.9 ± 8.7%; PP^+, 100 ± 12.5 vs. 105.0 ± 9.9%). Because the total number of islet cells did not change (Fig. 3.5), the increased PP^+ cells could have differentiated from Arx^+/Glu^- precursor cells. In summary, the population change is likely not due to cell fate conversion, rather to alterations in cell fate specification during the developmental stage, highlighting the importance of MafB for α-cell lineage specification due to its suppression of PP-cell fate differentiation (Fig. 4.3).

4-3. Discussion

Interestingly, the population of PP^+ cells was increased at the expense of the decreased population of α-cells. During early pancreas morphogenesis, α/PP precursor cells (Arx^+) preferentially differentiate towards the α-cell lineage, while a few cells are designated into PP-cell fate (19, 38). However, in the *Mafb*$^{\Delta Endo}$ mice, a significant population of Arx^+/Glu^- cells are differentiated into PP-producing cells at 3 weeks of age, and their fate was maintained throughout the developmental stage until 8 weeks of age (Fig. 4.1C - F). Thus, α/PP precursor cells might favor promoting PP-cell lineage differentiation in the absence of MafB, indicating that MafB plays a potential role in the early α-cell fate decision during islet development by inhibiting PP cell differentiation (Fig. 4.3).

4-4. Materials and Methods

Immunohistochemistry

The pancreatic tissues were fixed overnight in 4% paraformaldehyde (PFA) in phosphate-buffered saline (PBS) at 4°C, processed, and embedded in paraffin. Then, 2-μm sections were sliced and prepared according to standard methods. For the nuclear protein staining, the sections were soaked in 0.3% Triton X-100/PBS solution, followed by heat-induced epitope retrieval using Target Retrieval Solution (Dako) and a pressure cooker. All sections were blocked with appropriate serum for 1 h at room temperature and incubated overnight at 4°C with the following primary antibodies: guinea pig anti-insulin (1:500; ab7842, Abcam), guinea pig anti-glucagon (1:1000; M182, Takara), rabbit anti-Arx (1:250; generous gift from Drs. Kunio Kitamura and Ken-ichirou Morohashi, Kyushu University, JAPAN) (26), rabbit anti-pancreatic polypeptide (1:1000; ab113694, Abcam), goat anti-pancreatic polypeptide (1:50; ab77192, Abcam) and rabbit anti-somatostatin (1:50; 18-007, Zymed). The antigens were visualized using appropriate secondary antibodies conjugated to Alexa Flour 488 or 594 (1:1000; Life Technologies), and the nuclei were labeled with Hoechst 33342 (Molecular Probes). The tissue specimens were mounted with Fluoromount (Diagnostic BioSystems). All images were acquired under a fluorescence microscope (BIOREVO BZ-9000, Keyence).

Cell counting

Following the immunofluorescence staining, the numbers of different cell types in the islet microscopy images of each islet were manually counted. For each cell type, 20-40 representative islets from 3-6 mice per group were counted. To calculate the fraction of Som^+ and PP^+ cells within the islet, the number of Som^+ and PP^+ cells per

islet was manually counted using ImageJ software and divided by the total number of Hoechst^{+} nuclei from the same islet (% hormone^{+} cells/islet Hoechst^{+} nuclei) and then normalized to the control group.

Statistical analysis

All data are presented as the mean ± SEM. To determine the statistical significance between the MafB mutants and controls, a minimum of three biological replicates were analyzed by performing Welch's *t*-test, and a p-value < 0.05 was considered significant.

4-5. Figures and Legends

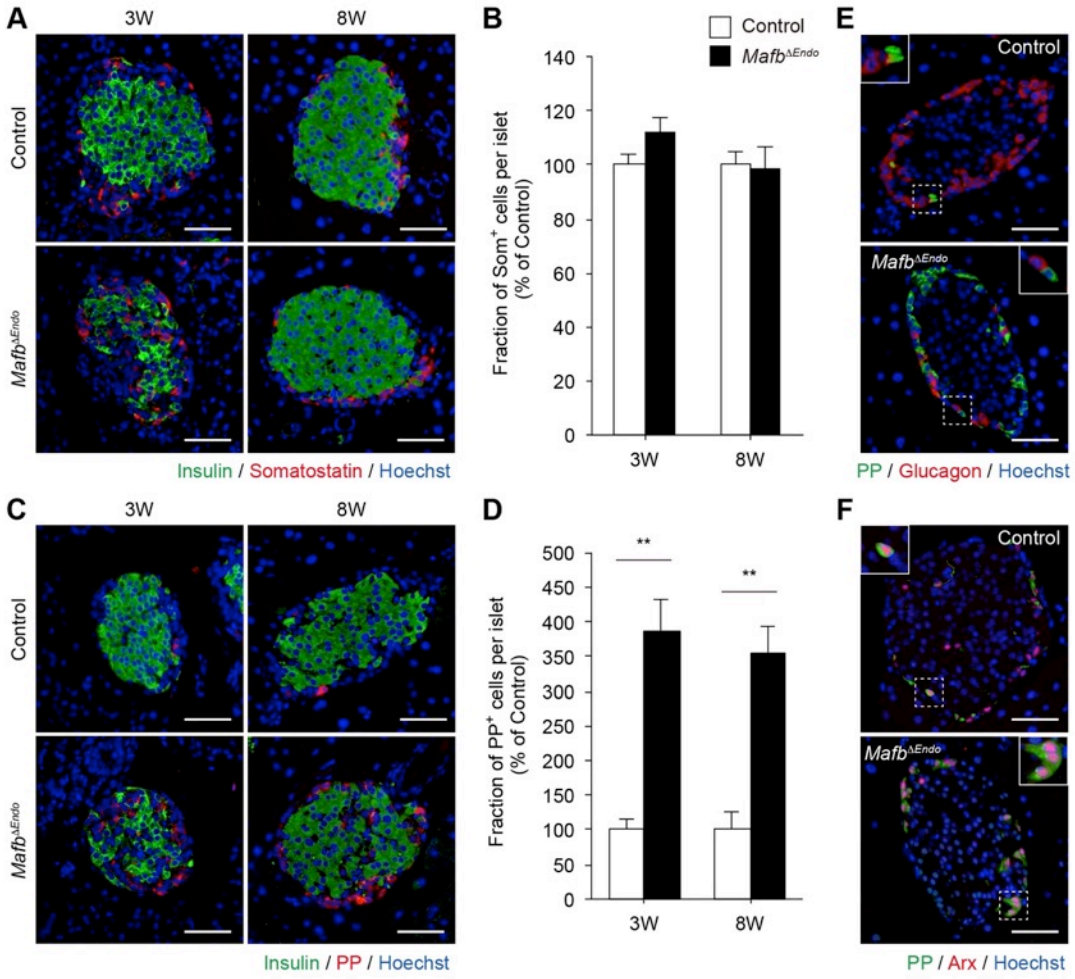

Fig. 4.1 PP$^+$ cell population is increased in the *Mafb$^{\Delta Endo}$* pancreas.

(A) Immunostaining of insulin (green) with somatostatin (Som, red) and **(C)** pancreatic polypeptide (PP, red) in *Mafb$^{\Delta Endo}$* and control (*Mafb$^{f/f}$*) pancreata from 3- and 8-week-old animals. Nuclei were stained with Hoechst 33342. Scale bars, 50 μm. **(B)** Fraction of Som$^+$ and **(D)** PP$^+$ cells within islets in *Mafb$^{\Delta Endo}$* (closed bars) and control (open bars) pancreata (n ≥ 4). ** $p < 0.01$. **(E)** Investigation of cell fate conversion by co-staining PP (green) with glucagon (red) or **(F)** Arx (red) antibodies in *Mafb$^{\Delta Endo}$* and control pancreata from 8-week-old animals. Nuclei were stained with Hoechst 33342. Scale bars, 50 μm.

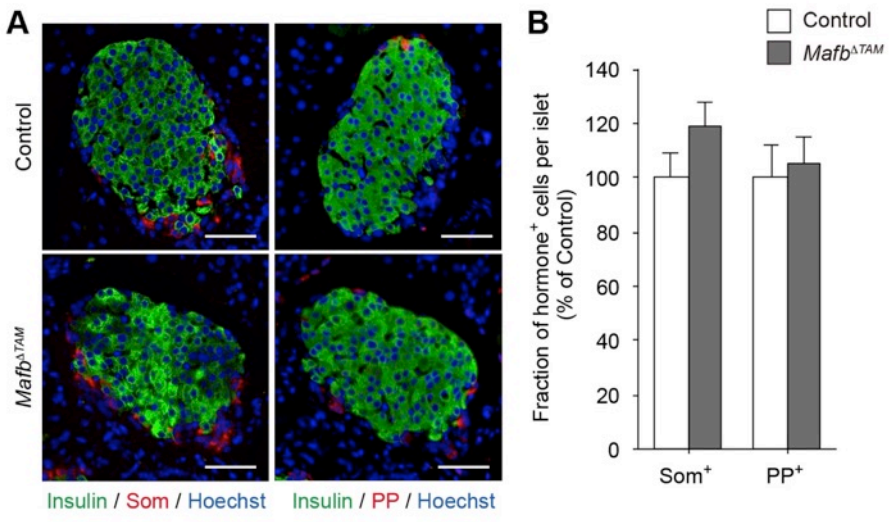

Fig. 4.2. *Mafb* deletion after islet maturation does not affect δ- and PP-cell.

(A) Immunostaining of insulin (green) with somatostatin (Som; left panels, red) and pancreatic polypeptide (PP; right panels, red) in $Mafb^{\Delta TAM}$ and control ($Mafb^{f/f}$) mice 11 weeks post-tamoxifen (TAM) injection. TAM was injected at 5 weeks of age. Nuclei were stained with Hoechst 33342. Scale bars, 50 μm. **(B)** Fraction of Som^+ and PP^+ cells within islets in $Mafb^{\Delta TAM}$ (closed bars) and control (open bars) pancreata ($n \geq 4$) from 11 weeks post-injection animals.

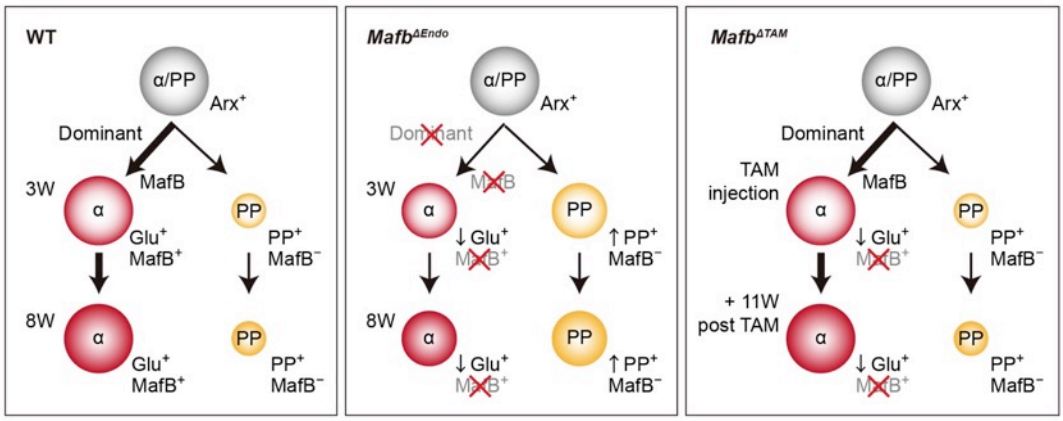

Fig. 4.3. Model of α- and PP-cell lineage differentiation.

Schematic model of α- and PP-cell lineage specification from the α/PP precursor cells in wild-type (WT), *Mafb*$^{\Delta Endo}$, and *Mafb*$^{\Delta TAM}$ mice.

CHAPTER 5:

The role of MafB in glucagon regulation

5-1. Purpose

According to the results from previous chapters, MafB is important for both α- and β-cell development at the neonatal stage and critical for the maintenance of glucagon production in α-cells. Here, I future explore the MafB-regulated genes that are involved in α- and β-cell differentiation as well as hormone production and secretion by performing a real-time qPCR analysis of pancreatic islet cDNA.

5-2. Results

MafB is a key regulator of glucagon gene expression.

Islets were isolated from 10-week-old *Mafb*$^{\Delta Endo}$ and TAM-injected *Mafb*$^{\Delta TAM}$ mice 3 weeks post-injection. The mRNA expression analysis revealed successful deletion of *Mafb* in both mutant models (Fig. 5.1A and B) and the consequent decrease in glucagon gene (*Gcg*) expression (Fig. 5.1C and D). The *Mafb*$^{\Delta Endo}$ islets exhibited a marked decrease in *Arx* transcription that was equivalent to the reduced number of Arx^{+} cells observed via immunohistochemistry (Fig. 2.4E), while a moderate decrease in the expression of *Brn4*, which is another α-cell-enriched gene (14), was also observed (Fig. 5.1C). In addition, the expression of β-cell-enriched genes (i.e., *Ins2*, *Pdx1*, and *Nkx6.1*) (14) was significantly lower in the *Mafb*$^{\Delta Endo}$ islets (Fig. 5.1C), which could explain the partial recovery of insulin production indicated by the slight reduction in the Ins^{+} cell population and insulin content (Fig. 2.2B and E). Thus, these results support my conclusion that an *Mafb* deficiency during embryogenesis suppresses α-cell development and glucagon expression and delays β-cell terminal differentiation. Moreover, the increase in the PP^{+} cell population in the *Mafb*$^{\Delta Endo}$ mice was further supported by an up-regulated *Ppy*

mRNA level in the islets (Fig. 5.1C). Interestingly, the *Mafb*$^{\Delta Endo}$ islets also showed decreased expression of the ghrelin gene (*Ghrl*) (Fig. 5.1C). Because certain ghrelin^{+} cells express MafB in wild-type embryos and neonatal mice pancreas (10, 39), the *Mafb* depletion during the embryonic stage may have affected the development of the ghrelin^{+} cell subpopulation. In contrast, the *Mafb*$^{\Delta TAM}$ islets did not display any differences in the expression of α- and β-cell-enriched genes (i.e., *Arx*, *Brn4*, *Ins2*, *Pdx1*, and *Nkx6.1*) or any other islet hormone genes (i.e., *Sst*, *Ppy*, and *Ghrl*) (Fig. 5.1D) (14), which is consistent with the immunostaining results (Fig. 3.2B, 3.4B and E). These data confirm that an *Mafb* ablation in adult mice impairs glucagon expression in α-cells but does not affect other islet cells.

Because the previous study has shown that the expression of glucagon fully recovers following *Mafb* deletion (10), I aimed to identify the compensatory mechanism of glucagon production in the absence of *Mafb*. Thus, I further inspected the gene expression levels of other transcription factors known to regulate glucagon and/or α-cell differentiation, including *Pax6* (40), *Foxa2* (41, 42), *Nkx2.2* (43), and the peptide-processing gene *Pcsk2* (44) that liberates glucagon from proglucagon. Two of the four glucagon/α-cell regulatory genes (i.e., *Foxa2* and *Nkx2.2*) were significantly reduced in the *Mafb*$^{\Delta Endo}$ islets, while the other two genes (i.e., *Pax6* and *Pcsk2*) exhibited a trend of reduced expression compared with that in the controls (Fig. 5.1E). Thus, the *Mafb* deletion in the developing endocrine cells led to a down-regulation of the other glucagon/α-cell regulators, which, in turn, exacerbated the glucagon reduction. Nevertheless, I cannot exclude the possibility that β-cells had an effect because these factors are also highly conserved in β-cells (14) and the *Mafb*$^{\Delta Endo}$ islets showed a decreased trend of β-cell-enriched gene expression (Fig.

5.1C). However, in the *Mafb*$^{\Delta TAM}$ islets, none of the glucagon/α-cell regulator genes were affected (Fig. 5.1F), suggesting that MafB is a major controller of α-cell functional maintenance in adult mice independent of other glucagon/α-cell regulators, such as Pax6, Foxa2, Nkx2.2, and Pcsk2. If these unaffected genes represent the α-cell population, then this could explain the residual glucagon production in the *Mafb*-deficient animals (*Mafb*$^{\Delta Endo}$ and *Mafb*$^{\Delta TAM}$) (Fig. 2.2F and 3.2E).

***Mafb* deletion disrupts glucagon secretion in response to α-cell stimuli.**

To address the functional competence of *Mafb*-deficient α-cells, I analyzed glucagon secretion in response to amino acid stimulation (45) in both mutant mice. Eight-week-old *Mafb*$^{\Delta Endo}$ and TAM-injected *Mafb*$^{\Delta TAM}$ male mice 3 weeks post-TAM treatment were injected with 1 mg/g L-arginine intraperitoneally after overnight fasting (Fig. 5.2A and B). In the basal state, the basal plasma glucagon levels in both mutant groups were significantly lower when compared with the control groups (Fig. 5.2A and B; Control vs. *Mafb*$^{\Delta Endo}$, 15.7 ± 2.1 vs. 8.6 ± 1.3 pg/ml; Control vs. *Mafb*$^{\Delta TAM}$, 17.0 ± 2.8 vs. 8.3 ± 1.8 pg/ml). These results likely reflect the constantly observed reduced glucagon production phenotype and highlight the importance of MafB in maintaining the basal glucagon production and secretion. After the arginine stimulation, a rapid increase in the plasma glucagon levels was observed within 2 min, and a peaked was observed 10 min after the arginine administration in all control groups (Fig. 5.2A and B). However, both *Mafb*-deficient mice failed to secrete glucagon at the control level, although the *Mafb*$^{\Delta TAM}$ mice exhibited slightly higher levels (Fig. 5.2A and B). Moreover, the plasma glucagon level peaked 2 min after the arginine injection in both mutants and remained unaltered (Fig. 5.2A and B),

suggesting the presence of possible defects in the cellular machinery that regulates glucagon secretion.

To test whether arginine uptake via cationic amino acid transporters and/or the glucagon-secreting machinery was affected, real-time qPCR was performed on isolated pancreatic islets from 10-week-old *Mafb*$^{\Delta Endo}$ and *Mafb*$^{\Delta TAM}$ mice 3 weeks post-TAM injection. Since the β-cells were persistently affected by the *Mafb* ablation in the *Mafb*$^{\Delta Endo}$ mice, both cationic amino acid transporter genes (i.e., *Slc7a1* and *Slc7a2*) and K^{ATP} channel subunit genes (i.e., *Kir6.2* and *Sur1*) involved in glucagon secretion (45) were down-regulated (Fig. 5.2C). However, the *Mafb*$^{\Delta TAM}$ islets exhibited significant reductions in *Slc7a1* and *Slc7a2* but not *Kir6.2* and *Sur1* (Fig. 5.2D). Therefore, the impaired arginine-stimulated glucagon secretion likely reflects reduced cationic amino acid transporter gene expression in both mutants and can be partially attributed to the reduced K^{ATP} channel subunits in the *Mafb*$^{\Delta Endo}$ mice. Overall, these data suggest that *Mafb* ablation leads to insufficient glucagon secretion under basal and stimulated conditions, thereby supporting the role of MafB in α-cell development and function.

5-3. Discussion

This study confirmed my conclusion that MafB is important for α- and β-cell development and is critical for glucagon expression in α-cell *in vivo*. Both the *Mafb*$^{\Delta Endo}$ and *Mafb*$^{\Delta TAM}$ islets showed nearly complete deletion of *Mafb* expression and the consequent down-regulation of the glucagon gene expression. In the *Mafb*$^{\Delta TAM}$ islets, no apparent changes were observed in the expression of α- and β-cell-enriched genes or the glucagon/α-cell regulatory genes. Collectively, the qPCR data support

the hypothesis that MafB substantially regulates glucagon gene expression *in vivo* and is a principal regulator of the glucagon gene.

Given the recovery of the α-cell numbers and glucagon content in the *Mafb*$^{\Delta panc}$ mice (10), I further explored the secondary effects on glucagon production in the absence of *Mafb*, which indeed was constantly observed in both mutant mice (Fig. 2.4G and 3.4G). Various transcription factors, including MafB (9), c-Maf (46), Pax6 (40), Foxa1, Foxa2 (41, 42), NeuroD1 (47), Isl1 (48), and Brn4 (49), have been reported to regulate glucagon expression in α-cells. However, MafB and Brn4 are the only two factors known to be α-cell-specific, whereas the other genes are expressed in both α- and β-cells (14). Interestingly, a previous study investigating *Brn4*-null mice observed no significant impact on glucagon gene expression, synthesis, and secretion, suggesting that Brn4 is dispensable in glucagon regulation (50). In contrast, the relationship between MafB and glucagon expression has been clearly illustrated (38, 51). For example, both the overexpression of *Arx* in pancreatic-progenitor cells and the deletion of *Pdx1* in the β-cells lead to an increase in the α-cell population, which is frequently associated with MafB and glucagon expression (38, 51). Thus, MafB likely dominates the regulation of α-cell activity, including glucagon production and secretion, although a minimal level of glucagon is maintained through an MafB independent pathway. According to the *Mafb*$^{\Delta TAM}$ islet gene analysis, the mRNA levels of *Pax6*, *Foxa2*, *Nkx2.2*, and *Pcsk2* remained unchanged, with no indication of rescuing the depleted glucagon gene expression (Fig. 5.1F). Thus, *Mafb* ablation was exclusively responsible for glucagon reduction, supporting my hypothesis that MafB is the principal transcriptional activator of the glucagon gene in α-cells.

Although α-cell dysfunction is distinctly addressed in a study by Conrad *et al.*, the specific glucagon secretary machinery affected by the *Mafb* ablation was not identified (10). In both of my mutant mice, cationic amino acid transporter genes (i.e., *Slc7a1* and *Slc7a2*) are significantly decreased (Fig. 5.2C and D), suggesting that impaired arginine-stimulated glucagon secretion is likely caused by the reduced arginine transporter gene expression. Based on the Text Mining Application from SABiosciences and the UCSC Genome Browser, Foxa2 is predicted to target these transporter genes. However, *Foxa2* expression was not reduced according to my qPCR analysis (Fig. 5.1F), indicating that the reduction in *Slc7a1* and *Slc7a2* expression is independent of Foxa2 and that an alternative mechanism is responsible for the regulation of cationic amino acid transporter gene expression.

Understanding α-cell functional activity not only enhances our knowledge of islet physiology but also has translational implications, given that the regulation of glucagon secretion and action have been shown to ameliorate diabetes symptoms (52, 53). Extremely high plasma glucagon concentrations are observed in insulin-deficient states, such as type 1 diabetes, advanced type 2 diabetes and diabetic ketoacidosis (2, 54). Therefore, inhibiting glucagon signaling may potentially reduce diabetic hyperglycemia, as demonstrated in animal studies. For example, compared with control mice, mice with either a disrupted glucagon receptor (55, 56) or defective glucagon synthesis (57, 58) tend to display reduced fasting blood glucose levels and improved glucose tolerance, even without treatment. Furthermore, glucagon receptor-knockout mice are resistant to diabetes upon streptozotocin (STZ)-induced β-cell destruction (59). In addition, a recent study using a peptide-based glucagon receptor antagonist reported an improved metabolic control of genetically or directly induced

obesity-related diabetes in mice (60). Therefore, my discovery may potentiate glucagon regulation in diabetes through *Mafb* gene regulation.

5-4. Materials and Methods

Isolation of pancreatic islets

Pancreatic islets were isolated from 10-week-old $Mafb^{\Delta Endo}$ and $Mafb^{\Delta TAM}$ mice 3 weeks post-TAM injection as previously described with slight modifications (61). Briefly, after clamping the common bile duct at the intestine, the pancreas was inflated with 1 mg/ml collagenase type V (Wako) diluted in Krebs-Ringer Bicarbonate (KRBH) buffer (129.4 mM NaCl, 5.2 mM KCl, 1.3 mM KH_2PO_4, 1.3 mM $MgSO_4$, 2.7 mM $CaCl_2$, 24.8 mM $NaHCO_3$, 10 mM HEPES; pH 7.4). The distended pancreas was transferred to a collecting tube containing additional fresh collagenase solution and then incubated at 37˚C for 20 min with gentle shaking. After the second wash with ice-cold KRBP buffer containing 0.5% bovine serum albumin (BSA), the islets were hand-picked under a stereomicroscope.

Quantitative real-time PCR (qPCR)

Total RNA was extracted in ISOGEN (Nippon gene) from isolated pancreatic islets of 10-week-old $Mafb^{\Delta Endo}$ and $Mafb^{\Delta TAM}$ mice 3 weeks post-TAM injection. cDNA was synthesized according to the protocol of the QuantiTect Reverse Transcription Kit (Qiagen). Real-Time qPCR reactions were performed in duplicate on a Thermal Cycler Dice Real-Time System (Takara) using SYBR Green PCR master mix (Takara). The expression of all target genes was normalized to that of *Hprt*. The primers used in this study are listed in Table 1.

Arginine-stimulated glucagon secretion

Eight-week-old *Mafb*$^{\Delta Endo}$ and *Mafb*$^{\Delta TAM}$ male mice 3 weeks post-TAM injection, and their corresponding controls were fasted for 16 h overnight. On the following morning, 1 mg/g body weight of L-arginine (Sigma) was injected intraperitoneally, and venous blood was collected at 0, 2, 10, and 25 min post-injection into heparinized tubes (Drummond Scientific Company). The plasma glucagon levels were determined using the Mercodia Glucagon 10 µl ELISA Kit (10-1281-01).

Statistical analysis

All data are presented as the mean ± SEM. To determine the statistical significance between the MafB mutants and controls, a minimum of three biological replicates were analyzed by performing Welch's *t*-test, and a p-value < 0.05 was considered significant. To compare the longitudinal data obtained from the arginine-stimulated glucagon secretion test, the *p*-values were calculated using Welch's *t*-test followed by Holm's correction for multiple comparisons.

Table 1. Primer sequences used for the real-time qPCR analysis.

Gene	Primer Sequences (5' → 3')	
	Forward Primer	Reverse Primer
Hprt	ttgttgttggatatgcccttgacta	aggcagatggccacaggacta
Mafb	tgaatttgctggcactgctg	aagcaccatgcggttcataca
Gcg	agggacctttaccagtgatgt	aatggcgacttcttctgggaa
Arx	tccggataccccacttagctt	gacgccccttttcctttaagtg
Brn4	ctcgccgcacactaaccat	gctccagcataccgctcac
Ins2	gcttcttctacacacccatgtc	agcactgatctacaatgccac
Pdx1	ttcccgaatggaaccgagc	gtaggcagtacgggtcctct
Nkx6.1	cagacccacgttctctggac	tgacctgactctccgtcatcc
Sst	gagcccaaccagacagagaa	gaagttcttgcagccagctt
Ppy	tactgctgcctctccctgtt	ccaggaagtccacctgtgtt
Ghrl	gaagccaccagctaaactgc	gcctgtccgtggttacttgt
Pax6	atatgtcgacagctccagcatgcagaac	tgcccagaattttactcacacaa
Foxa2	gagcaccattacgccttcaac	aggccttgaggtccattttgt
Nkx2.2	atgtcgctgaccaacacaaa	tcaccggacaatgacaagga
Pcsk2	aatgacccctacccataccc	gaggaggcttcgatgatgtc
Kir6.2	gtaggggacctccgaaagag	tggagtcgatgacgtggtag
Sur1	ctggtcctcagcagcacat	ggaactcttgggacgagaca
Slc7a1	atcggtacttcaagcgtggc	ccatggctgactccttcacg
Slc7a2	atggctttacagggacgttg	gcgttaaagctgcagaaacc

5-5. Figures and Legends

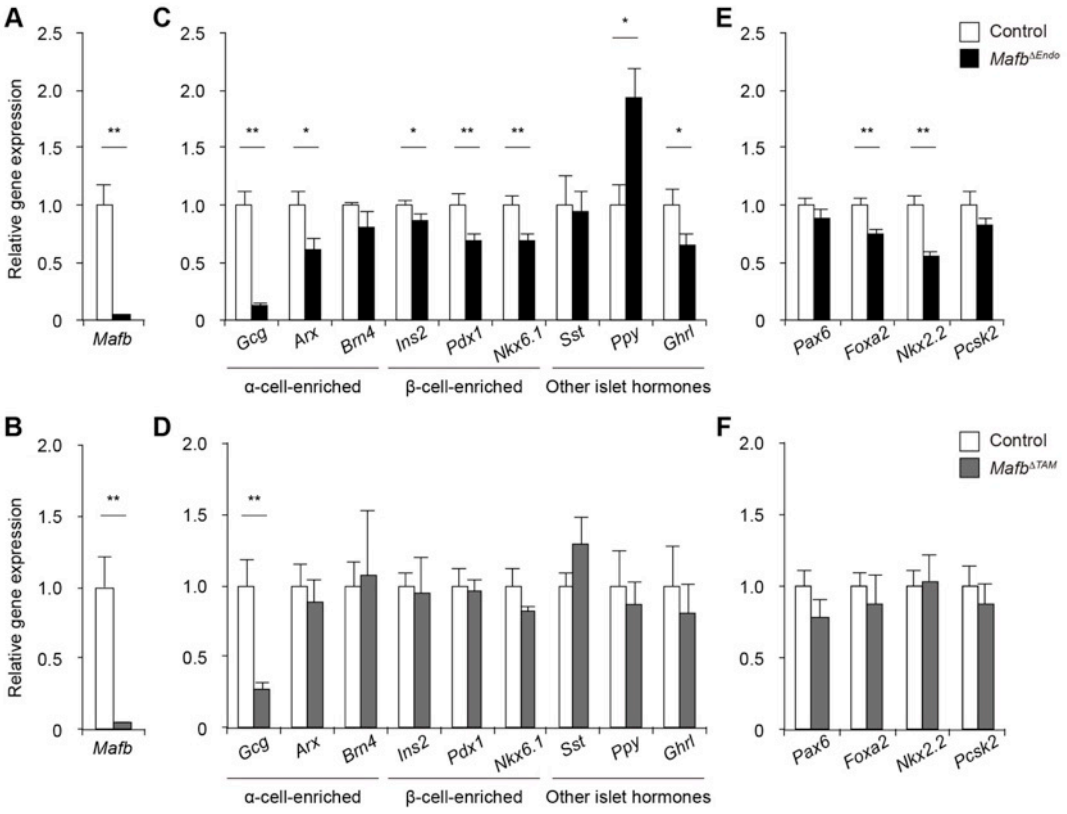

Fig. 5.1 MafB is a key regulator of glucagon expression.

Gene expression comparisons were performed by a qPCR analysis of pancreatic islets isolated from 10-week-old *Mafb*$^{\Delta Endo}$ (upper panels) and *Mafb*$^{\Delta TAM}$ mice 3 weeks post-tamoxifen (TAM) injection (bottom panels) ($n \geq 5$). TAM was injected at 5 weeks of age. **(A and B)** *Mafb* gene, **(C and D)** islet hormone and cell identity genes, and **(E and F)** glucagon production/α-cell differentiation regulatory genes were analyzed. Primers are listed in Table 1. * $p < 0.05$ and ** $p < 0.01$.

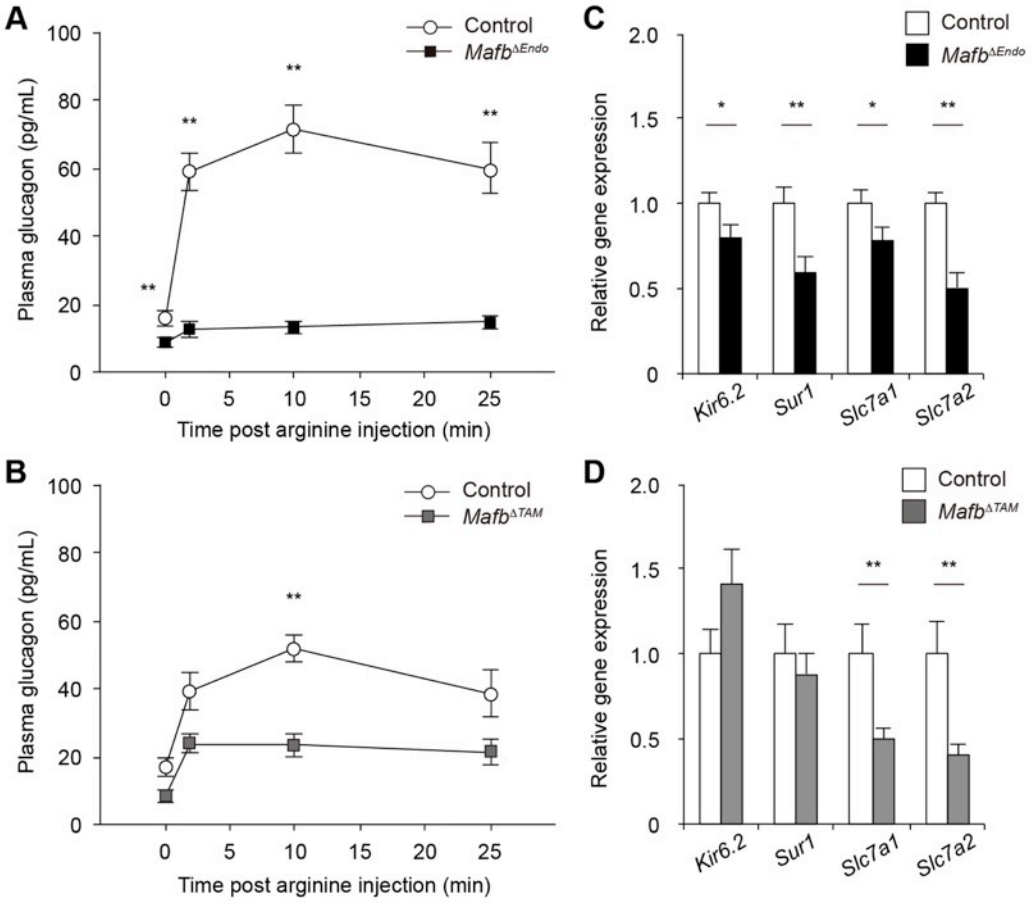

Fig. 5.2 *Mafb* deletion impairs glucagon secretion upon α-cell stimulation.

(A and B) Glucagon secretion was measured after an intraperitoneal injection of L-arginine (1 mg/g body weight) in **(A)** 8-week-old $Mafb^{\Delta Endo}$ ($n \geq 8$) and **(B)** $Mafb^{\Delta TAM}$ male mice 3 weeks post-tamoxifen (TAM) administration ($n \geq 4$). TAM was injected at 5 weeks of age. ** $p < 0.01$. **(C and D)** qPCR analysis of glucagon secretion machinery gene expression was performed on pancreatic islets isolated from **(C)** 10-week-old $Mafb^{\Delta Endo}$ and **(D)** $Mafb^{\Delta TAM}$ mice 3 weeks post-TAM injection ($n \geq 5$). * $p < 0.05$ and ** $p < 0.01$.

CHAPTER 6:

SUMMARY AND CONCLUSION

6-1. Summary

In the present study, I demonstrate that MafB regulates glucagon production and secretion in postnatal α-cells *in vivo* by using the following two different mouse models: endocrine cell-specific (*Mafb*$^{\Delta Endo}$) and TAM-dependent (*Mafb*$^{\Delta TAM}$) *Mafb* knockout mice. Both *Mafb*$^{\Delta Endo}$ and *Mafb*$^{\Delta TAM}$ mice exhibited a decreased population of Glu^{+} α-cells (Fig. 2.2C and 3.2C) and, consequently, reduced glucagon production (Fig. 2.3B and 3.3B) and secretion (Fig. 5.2A and B). Although the α-cell fate was unchanged, embryonic *Mafb* deletion further reduced the Arx^{+} cell population (Fig. 2.5B) and increased the PP^{+} cell population to compensate for the decreased α-cell differentiation (Fig. 5B). Moreover, both mutant mice failed to respond to arginine (Fig. 5.2A and B), potentially due to the compromised expression of cationic amino acid transporter genes involved in arginine uptake (Fig. 5.3A and B). Therefore, my findings clearly demonstrate the contribution of MafB to α-cell development during the neonatal stage and the maintenance of α-cell function during adulthood *in vivo*.

6-2. Conclusion

In conclusion, my findings indicate that MafB is critical for glucagon production in α-cells to maintain development and function. Therefore, this study yields insight into islet physiology in glucagon regulation through MafB in α-cells, thereby providing a platform for understanding glucagon control under pathophysiological conditions.

REFERENCES

1. Unger RH, Aguilar-Parada E, Müller WA, Eisentraut AM. 1970. Studies of pancreatic α cell function in normal and diabetic subjects. J Clin Invest 49:837–848.

2. Dunning BE, Gerich JE. 2007. The role of α-cell dysregulation in fasting and postprandial hyperglycemia in type 2 diabetes and therapeutic implications. Endocr Rev 28:253–283.

3. Menge BA, Grüber L, Jørgensen SM, Deacon CF, Schmidt WE, Veldhuis JD, Holst JJ, Meier JJ. 2011. Loss of inverse relationship between pulsatile insulin and glucagon secretion in patients with type 2 diabetes. Diabetes 60:2160–2168.

4. Benitez CM, Goodyer WR, Kim SK. 2012. Deconstructing pancreas developmental biology. Cold Spring Harb Perspect Biol 4:a012401.

5. van der Meulen T, Huising MO. 2015. Role of transcription factors in the transdifferentiation of pancreatic islet cells. J Mol Endocrinol 54:R103-117.

6. Zhang C, Moriguchi T, Kajihara M, Esaki R, Harada A, Shimohata H, Oishi H, Hamada M, Morito N, Hasegawa K, Kudo T, Engel JD, Yamamoto M, Takahashi S. 2005. MafA is a key regulator of glucose-stimulated insulin secretion. Mol Cell Biol 25:4969–4976.

7. Nishimura W, Kondo T, Salameh T, El Khattabi I, Dodge R, Bonner-Weir S, Sharma A. 2006. A switch from MafB to MafA expression accompanies differentiation to pancreatic β-cells. Dev Biol 293:526–539.

8. Artner I, Hang Y, Mazur M, Yamamoto T, Guo M, Lindner J, Magnuson MA, Stein R. 2010. MafA and MafB regulate genes critical to β-cells in a unique temporal manner. Diabetes 59:2530–2539.

9. Artner I, Le Lay J, Hang Y, Elghazi L, Schisler JC, Henderson E, Sosa-Pineda B, Stein R. 2006. MafB: an activator of the glucagon gene expressed in developing islet α- and β-cells. Diabetes 55:297–304.

10. Conrad E, Dai C, Spaeth J, Guo M, Cyphert HA, Scoville D, Carroll J, Yu W-M, Goodrich L V., Harlan DM, Grove KL, Roberts CT, Powers AC, Gu G, Stein R. 2015. The MAFB transcription factor impacts islet α-cell function in

rodents and represents a unique signature of primate islet β-cells. Am J Physiol - Endocrinol Metab 310:E91–E102.

11. Artner I, Blanchi B, Raum JC, Guo M, Kaneko T, Cordes S, Sieweke M, Stein R. 2007. MafB is required for islet β cell maturation. Proc Natl Acad Sci U S A 104:3853–3858.

12. Yoshida T, Ohkumo T, Ishibashi S, Yasuda K. 2005. The 5'-AT-rich half-site of Maf recognition element: a functional target for bZIP transcription factor Maf. Nucleic Acids Res 33:3465–3478.

13. Blanchi B, Kelly LM, Viemari J-C, Lafon I, Burnet H, Bévengut M, Tillmanns S, Daniel L, Graf T, Hilaire G, Sieweke MH. 2003. MafB deficiency causes defective respiratory rhythmogenesis and fatal central apnea at birth. Nat Neurosci 6:1091–1100.

14. Benner C, van der Meulen T, Cacéres E, Tigyi K, Donaldson CJ, Huising MO. 2014. The transcriptional landscape of mouse β cells compared to human β cells reveals notable species differences in long non-coding RNA and protein-coding gene expression. BMC Genomics 15:620.

15. Abdellatif AM, Ogata K, Kudo T, Xiafukaiti G, Chang Y-H, Katoh MC, El-Morsy SE, Oishi H, Takahashi S. 2015. Role of large MAF transcription factors in the mouse endocrine pancreas. Exp Anim 64:305–312.

16. Yoshida S, Takakura A, Ohbo K, Abe K, Wakabayashi J, Yamamoto M, Suda T, Nabeshima YI. 2004. Neurogenin3 delineates the earliest stages of spermatogenesis in the mouse testis. Dev Biol 269:447–458.

17. Hasegawa Y, Daitoku Y, Sekiguchi K, Tanimoto Y, Mizuno-Iijima S, Mizuno S, Kajiwara N, Ema M, Miwa Y, Mekada K, Yoshiki A, Takahashi S, Sugiyama F, Yagami K. 2013. Novel ROSA26 Cre-reporter knock-in C57BL/6N mice exhibiting green emission before and red emission after Cre-mediated recombination. Exp Anim 62:295–304.

18. Sander M, Sussel L, Conners J, Scheel D, Kalamaras J, Dela Cruz F, Schwitzgebel V, Hayes-Jordan A, German M. 2000. Homeobox gene Nkx6.1 lies downstream of Nkx2.2 in the major pathway of β-cell formation in the pancreas. Development 127:5533–5540.

19. Collombat P, Mansouri A, Hecksher-Sorensen J, Serup P, Krull J, Gradwohl G, Gruss P. 2003. Opposing actions of Arx and Pax4 in endocrine pancreas development. Genes Dev 17:2591–2603.

20. Gu G, Dubauskaite J, Melton DA. 2002. Direct evidence for the pancreatic lineage: NGN3+ cells are islet progenitors and are distinct from duct progenitors. Development 129:2447–2457.

21. Tran MTN, Hamada M, Nakamura M, Jeon H, Kamei R, Tsunakawa Y, Kulathunga K, Lin Y-Y, Fujisawa K, Kudo T, Takahashi S. 2016. MafB deficiency accelerates the development of obesity in mice. FEBS Open Bio 6:540–547.

22. Shichita T, Ito M, Morita R, Komai K, Noguchi Y, Ooboshi H, Koshida R, Takahashi S, Kodama T, Yoshimura A. 2017. MAFB prevents excess inflammation after ischemic stroke by accelerating clearance of damage signals through MSR1. Nat Med 23:723–732.

23. Yu W-M, Appler JM, Kim Y-H, Nishitani AM, Holt JR, Goodrich L V. 2013. A Gata3-Mafb transcriptional network directs post-synaptic differentiation in synapses specialized for hearing. Elife 2:e01341.

24. van der Meulen T, Mawla AM, DiGruccio MR, Adams MW, Nies V, Dólleman S, Liu S, Ackermann AM, Cáceres E, Hunter AE, Kaestner KH, Donaldson CJ, Huising MO. 2017. Virgin β cells persist throughout life at a neogenic niche within pancreatic islets. Cell Metab 25:911–926.e6.

25. Cheng Y, Kang H, Shen J, Hao H, Liu J, Guo Y, Mu Y, Han W. 2015. β-cell regeneration from vimentin+/MafB+ cells after STZ-induced extreme β-cell ablation. Sci Rep 5:11703.

26. Kitamura K, Yanazawa M, Sugiyama N, Miura H, Iizuka-Kogo A, Kusaka M, Omichi K, Suzuki R, Kato-Fukui Y, Kamiirisa K, Matsuo M, Kamijo S, Kasahara M, Yoshioka H, Ogata T, Fukuda T, Kondo I, Kato M, Dobyns WB, Yokoyama M, Morohashi K. 2002. Mutation of ARX causes abnormal development of forebrain and testes in mice and X-linked lissencephaly with abnormal genitalia in humans. Nat Genet 32:359–369.

27. im Walde SS, Dohle C, Schott-Ohly P, Gleichmann H. 2002. Molecular target structures in alloxan-induced diabetes in mice. Life Sci 71:1681–1694.

28. Dai C, Brissova M, Hang Y, Thompson C, Poffenberger G, Shostak A, Chen Z, Stein R, Powers AC. 2012. Islet-enriched gene expression and glucose-induced insulin secretion in human and mouse islets. Diabetologia 55:707–718.

29. Guo S, Dai C, Guo M, Taylor B, Harmon JS, Sander M, Robertson RP, Powers AC, Stein R. 2013. Inactivation of specific β cell transcription factors in type 2 diabetes. J Clin Invest 123:3305–3316.

30. Scoville DW, Cyphert HA, Liao L, Xu J, Reynolds A, Guo S, Stein R. 2015. MLL3 and MLL4 methyltransferases bind to the MAFA and MAFB transcription factors to regulate islet β-cell function. Diabetes 64:3772–3783.

31. Dworschak GC, Draaken M, Hilger A, Born M, Reutter H, Ludwig M. 2013. An incompletely penetrant novel MAFB (p.Ser56Phe) variant in autosomal dominant multicentric carpotarsal osteolysis syndrome. Int J Mol Med 32:174–178.

32. Mehawej C, Courcet J-B, Baujat G, Mouy R, Gérard M, Landru I, Gosselin M, Koehrer P, Mousson C, Breton S, Quartier P, Le Merrer M, Faivre L, Cormier-Daire V. 2013. The identification of *MAFB* mutations in eight patients with multicentric carpo-tarsal osteolysis supports genetic homogeneity but clinical variability. Am J Med Genet Part A 161:3023–3029.

33. Park JG, Tischfield MA, Nugent AA, Cheng L, Di Gioia SA, Chan W-M, Maconachie G, Bosley TM, Summers CG, Hunter DG, Robson CD, Gottlob I, Engle EC. 2016. Loss of MAFB function in humans and mice causes Duane syndrome, aberrant extraocular muscle innervation, and inner-ear defects. Am J Hum Genet 98:1220–1227.

34. Hayashi S, McMahon AP. 2002. Efficient recombination in diverse tissues by a tamoxifen-inducible form of Cre: a tool for temporally regulated gene activation/inactivation in the mouse. Dev Biol 244:305–318.

35. Nagao M, Cheong CW, Olsen BR. 2016. Col2-Cre and tamoxifen-inducible Col2-CreER target different cell populations in the knee joint. Osteoarthr Cartil 24:188–191.

36. Metzger D, Chambon P. 2001. Site- and time-specific gene targeting in the mouse. Methods 24:71–80.

37. Huang YH, Sun MJ, Jiang M, Fu BY. 2009. Immunohistochemical localization of glucagon and pancreatic polypeptide on rat endocrine pancreas: coexistence in rat islet cells. Eur J Histochem 53:81–85.

38. Collombat P, Hecksher-Sørensen J, Krull J, Berger J, Riedel D, Herrera PL, Serup P, Mansouri A. 2007. Embryonic endocrine pancreas and mature β cells acquire α and PP cell phenotypes upon Arx misexpression. J Clin Invest 117:9610–9670.

39. Nishimura W, Rowan S, Salameh T, Maas RL, Bonner-Weir S, Sell SM, Sharma A. 2008. Preferential reduction of β cells derived from Pax6-MafB pathway in MafB deficient mice. Dev Biol 314:443–456.

40. St-Onge L, Sosa-Pineda B, Chowdhury K, Mansouri A, Gruss P. 1997. Pax6 is required for differentiation of glucagon-producing α-cells in mouse pancreas. Nature 387:406–409.

41. Kaestner KH, Katz J, Liu Y, Drucker DJ, Schütz G. 1999. Inactivation of the winged helix transcription factor HNF3α affects glucose homeostasis and islet glucagon gene expression in vivo. Genes Dev 13:495–504.

42. Gauthier BR, Schwitzgebel VM, Zaiko M, Mamin A, Ritz-Laser B, Philippe J. 2002. Hepatic nuclear factor-3 (HNF-3 or Foxa2) regulates glucagon gene transcription by binding to the G1 and G2 promoter elements. Mol Endocrinol 16:170–183.

43. Sussel L, Kalamaras J, Hartigan-O'Connor DJ, Meneses JJ, Pedersen RA, Rubenstein JL, German MS. 1998. Mice lacking the homeodomain transcription factor Nkx2.2 have diabetes due to arrested differentiation of pancreatic β cells. Development 125:2213–2221.

44. Furuta M, Zhou A, Webb G, Carroll R, Ravazzola M, Orci L, Steiner DF. 2001. Severe defect in proglucagon processing in islet α-cells of prohormone convertase 2 null mice. J Biol Chem 276:27197–27202.

45. Quesada I, Tudurí E, Ripoll C, Nadal A. 2008. Physiology of the pancreatic α-cell and glucagon secretion: role in glucose homeostasis and diabetes. J Endocrinol 199:5–19.

46. Gosmain Y, Avril I, Mamin A, Philippe J. 2007. Pax-6 and c-Maf functionally interact with the α-cell-specific DNA element G1 in vivo to promote glucagon gene expression. J Biol Chem 282:35024–35034.

47. Dumonteil E, Laser B, Constant I, Philippe J. 1998. Differential regulation of the glucagon and insulin I gene promoters by the basic helix-loop-helix transcription factors E47 and BETA2. J Biol Chem 273:19945–19954.

48. Wang M, Drucker DJ. 1995. The LIM domain homeobox gene isl-1 is a positive regulator of islet cell-specific proglucagon gene transcription. J Biol Chem 270:12646–12652.

49. Hussain MA, Lee J, Miller CP, Habener JF. 1997. POU domain transcription factor brain 4 confers pancreatic α-cell-specific expression of the proglucagon gene through interaction with a novel proximal promoter G1 element 17:7186–7194.

50. Hussain MA, Miller CP, Habener JF. 2002. Brn-4 transcription factor expression targeted to the early developing mouse pancreas induces ectopic glucagon gene expression in insulin-producing β cells. J Biol Chem 277:16028–16032.

51. Gao T, McKenna B, Li C, Reichert M, Nguyen J, Singh T, Yang C, Pannikar A, Doliba N, Zhang T, Stoffers DA, Edlund H, Matschinsky F, Stein R, Stanger BZ. 2014. Pdx1 maintains β cell identity and function by repressing an α cell program. Cell Metab 19:259–271.

52. Unger RH, Cherrington AD, Wollheim C, Wang Z, Unger R, Friedman J. 2012. Glucagonocentric restructuring of diabetes: a pathophysiologic and therapeutic makeover. J Clin Invest 122:4–12.

53. Sandoval DA, D'Alessio DA. 2015. Physiology of proglucagon peptides: role of glucagon and GLP-1 in health and disease. Physiol Rev 95:513–548.

54. Müller WA, Faloona GR, Unger RH, Faloona G, Unger R, Derot M. 1973. Hyperglucagonemia in diabetic ketoacidosis. Am J Med 54:52–57.

55. Parker JC, Andrews KM, Allen MR, Stock JL, McNeish JD. 2002. Glycemic control in mice with targeted disruption of the glucagon receptor gene. Biochem Biophys Res Commun 290:839–843.

56. Gelling RW, Du XQ, Dichmann DS, Romer J, Huang H, Cui L, Obici S, Tang B, Holst JJ, Fledelius C, Johansen PB, Rossetti L, Jelicks LA, Serup P, Nishimura E, Charron MJ. 2003. Lower blood glucose, hyperglucagonemia, and pancreatic α cell hyperplasia in glucagon receptor knockout mice. Proc Natl Acad Sci U S A 100:1438–1443.

57. Hancock AS, Du A, Liu J, Miller M, May CL. 2010. Glucagon deficiency reduces hepatic glucose production and improves glucose tolerance in adult mice. Mol Endocrinol 24:1605–1614.

58. Hayashi Y. 2011. Metabolic impact of glucagon deficiency. Diabetes, Obes Metab 13:151–157.

59. Lee Y, Wang M-Y, Du XQ, Charron MJ, Unger RH. 2011. Glucagon receptor knockout prevents insulin-deficient type 1 diabetes in mice. Diabetes 60:391–397.

60. O'Harte FPM, Franklin ZJ, Irwin N. 2014. Two novel glucagon receptor antagonists prove effective therapeutic agents in high-fat-fed and obese diabetic mice. Diabetes, Obes Metab 16:1214–1222.

61. Lacy PE, Kostianovsky M. 1967. Method for the isolation of intact islets of Langerhans from the rat pancreas. Diabetes 16:35–39.